Molecular Genetic Analysis of Mechanism for High Behavioral Stress Responses in Wild-derived Mice

20091854 Akira Tanave

Department of Genetics

School of Life Science

The Graduate University for Advanced Studies

2015/01/08

Publication list

(1) Toshiya Arakawa*, Akira Tanave*, Shiho Ikeuchi, Aki Takahashi, Satoshi Kakihara, Shingo Kimura, Hiroki Sugimoto, Nobuhiko Asada, Toshihiko Shiroishi, Kazuya Tomihara, Takashi Tsuchiya, Tsuyoshi Koide (2014). A male-specific QTL for social interaction behavior in mice mapped with automated pattern detection by a hidden Markov model incorporated into newly developed freeware. J Neurosci Methods. Advanced online. doi: 10.1111/gbb.12088. *Equally contributed.

(2) Tatsuhiko Goto, Akira Tanave, Kazuo Moriwaki, Toshihiko Shiroishi, Tsuyoshi Koide (2013). Selection for reluctance to avoid humans during the domestication of mice. Genes Brain Behav. 12(8): p.760-770. doi: 10.1111/gbb.12088.

1. Abstract

Behavioral responses to stress are tightly associated with physiological reaction. It is known that behavioral responses to stress have been decreased in domesticated animals during the breeding process of domestication. In house mice (*Mus musculus*), laboratory mice show lower behavioral responses to stress than wild mice given that the laboratory mice are originated in domesticated mice. However, actual genetic and molecular basis of the behavioral differences between laboratory and wild mice remained to be clarified.

Anxiety is one of the stress responses in human by expecting danger or awful situation in future. In animal models, anxiety-like behavior has been proposed as one type of behavioral responses to stress which are similar to human's anxiety responses. Previously, our group revealed that chromosome 17 is responsible for high anxiety-like behaviors using a panel of chromosome substitution (consomic) strains. A consomic strain, B6-ChrN^{MSM} (N indicates substituted chromosome number), is a mouse strain which has same genetic background as a laboratory strain C57BL/6 (B6), but only one of the chromosomes is replaced with the corresponding chromosome from a Japanese wild strain MSM/Ms (MSM). Given that B6-Chr17^{MSM} exhibits higher anxiety-like behaviors comparing to B6, it is speculated that the behavioral differences is caused by polymorphisms between B6 and MSM on the chromosome 17. However, actual causal genetic factor of the high anxiety-like behavior of the consomic strain had not been studied further from the chromosomal level. In order to address to the mechanisms associated with difference in anxiety-like behavior, I decided to conduct genetic and molecular analysis using B6-Chr17^{MSM}.

In Part I of this article, I report on my study for positional cloning of the gene related to the high anxiety-like behavior in B6-Chr17^{MSM} and on the results of further molecular analysis of the gene. In order to conduct genetic analysis of anxiety-like behaviors in an open-field, I

developed a series of sub-consomic strains, each of which carries partial segment of MSM-derived chromosome 17 from B6-Chr17^{MSM}. I mapped a genetic locus responsible for high anxiety-like behaviors in a region between D17Mit129 to the telomere end, the region is covered in sub-consomic T103 strain. In order to map the genetic locus with fine resolution, I developed further congenic strains from the sub-consomic T103 strain. I conducted open-field test using these congenic strains, and mapped the region into about 2.6 Mb segment at the distal part of chromosome 17, named as T116-T119 locus. Given that a gene which is a cause of high anxiety-like behaviors should be located in the T116-T119 locus, I searched for the possible candidate genes in the T116-T119 locus from a mouse genome database. I found only one protein-coding gene PACAP (pituitary adenylate cyclase activating polypeptide) as the candidate gene. PACAP is a neuropeptide which induces stress responses in hypothalamus. These results indicated that PACAP is a strong candidate for the high anxiety-like behavior of B6-Chr17^{MSM}.

PACAP has been implicated in anxiety-like behaviors that are decreased in PACAP knockout mice and enhanced by administration of PACAP into hypothalamus. Based on these previous reports, I characterized PACAP gene further at molecular level. I revealed that there is no difference at the nucleotide sequence of the coding region in PACAP gene between MSM and B6 alleles. In contrast, expression levels of PACAP gene in hypothalamus are significantly higher in the congenic strains which have MSM allele than that of B6. These results indicated that the high behavioral responses to stress in the congenic strains might be caused by the high PACAP expression.

In Part II of this article, I report on results of my study on genetic polymorphisms related to different expression of PACAP gene. In the sequence characterization of PACAP gene, I found a microsatellite (TG dinucleotide repeat) marker, D17Mit123, which is highly polymorphic among strains, in the non-coding region. It has been reported that some of the TG repeats in 5'-UTR

(untranslated region) act as enhancer or splicing regulator. I investigated the molecular function of the TG repeat in PACAP expression using *in vivo* and *in vitro* analyses. I found that long TG repeat length results in the high PACAP expression as well as decreased alternative splicing of 5'-untranslated exon 1B among in several mouse strains. These associations were further confirmed by luciferase assays using PACAP minigenes containing B6-derived $(TG)_{26}$ or MSM-derived $(TG)_{40}$. Interestingly, I found that the TG repeat lengths are clearly shorter in a group of laboratory strains than a group of wild strains, suggesting the association of the shorter TG repeat with domestication process. Taken together, I suggest that TG repeats can regulate PACAP expression via activities of enhancer and splicing regulators that might be associated with high behavioral responses to stress in wild mice.

2. PART I: Genetic mapping and candidate PACAP gene

2.1. Introduction

Stress responses affect animal behaviors through regulation of neuronal and hormonal networks. The major effects of them are mediated by hypothalamic-pituitary-adrenal (HPA) and spinal-sympathetic-adrenal-medullary (SAM) axes in which neuronal cells secrete and receive a variety of neurotransmitters that act as stimulatory or inhibitory substances on the system (Smith SM and Vale WW 2006, Ulrich-Lai YM and Herman JP 2009). In the HPA axis, stress responses lead to activation of corticotrophin-releasing hormone (CRH) neurons in the hypothalamic paraventricular nucleus (PVN) (Herman JP and Cullinan WE 1997). These neurons secrete CRH into the hypothalamo-pituitary portal system to stimulate pituitary adrenocorticotropic hormone (ACTH) secretion. ACTH arrives at adrenal cortex through the bloodstream, where it activates biosynthesis and release of glucocoriticoids.

The sensitivity to the stress depends on modifiable factors such as one's experience or environmental situation, but also on innate factors that can alter heritable nature such as genetic mutation and DNA methylation status. The genetic differences have been found in many genes including neuroendocrine-related genes such as peptide hormones (CRH, ACTH, AVP (arginine vasopressin), Neuropeptide Y (NPY), and so on) and its receptors (Zhou Z et al. 2008, Ising M and Holsboer F 2006, Makara GB et al. 2004, Schatzberg AF et al. 2014). In animal models, these genes have been reported to associate with behavioral responses to stress through neuroendocrinological pathways, especially for HPA axis (Bakshi VP and Kalin NH 2002, Steimer T 2011). However, these studies are not sufficient to understand the molecular mechanisms for which the sensitivities are different between individuals, as it could be caused by abnormal protein functions, high or low gene expressions, environmental various factors, or other mechanisms.

Domesticated house mice could provide a useful animal model to study the molecular mechanisms controlling the behavioral stress responses. There are several old literatures that illustrated or introduced a various coat color mutant mice that are often call as fancy mice (Tokuda M 1935). It is believed that these domesticated house mice had been developed by selecting tamed phenotype from wild mice by humans (Goto T et al. 2013). Well-studied domesticated house mice are classical laboratory mice derived from a few population bred from several crossing between European and Japanese fancy mice (Frazer KA et al. 2007). As in the case of other animals (Trut LN 1999), effects of the domestication process are reflected in reduced behavioral stress responses in the laboratory mice. In fact, the domestication from wild ancestors to the laboratory mice have decreased adrenal gland weights (Dunn TB and Andervont HB 1963, Badr FM et al. 1968), decreased corticosterone levels (Miller RA et al. 2000, Miller BH et al. 2010), and decreased immobility behaviors (pausing/freezing) (Blanchard RJ et al. 1998). These phenotypic differences will provide effective indexes to dissect the genetic differences between the wild and the laboratory mice.

The reduced behavioral stress responses can be observed as decreased anxiety-like behaviors in the laboratory mice (Takahashi A et al. 2006). Anxiety is one of the stress responses in humans, induced by expecting danger or awful situation in future. In the animal models, the anxiety-like behavior has been proposed as behavioral responses to stress which are similar to human's anxiety responses. In rodents, the anxiety-like behaviors can be observed as exploration, avoidance or immobilization based on their photophobicity (the tendency to prefer darkness and avoid bright areas), thigmotaxis/centrophobicity (the tendency to prefer edges and avoid open spaces), and neophilia (the tendency to prefer novel objects or environments) (Barnett SA 1958, 1963; Barnett SA and Cowan PE 1976; Calhoun JB 1962; Kerbusch JML et al. 1981). Open-field test has been frequently used as a behavioral test to measure the anxiety-like behaviors in rodents

(Hall CS and Ballachey EL 1932; Hall CS 1934, 1936a, 1936b). In the test, each animal is placed gently in a brightly lit field, which is a novel environment for the animal, and subsequent behaviors of the animal are recorded and analyzed. In the open field, the animal exhibits several characteristic behaviors such as leaning, rearing, pausing, and freezing. These behaviors have been used as indexes of the animal's anxiety in rodents (Makino J et al. 1991, Takahashi A et al. 2006, Takahashi A et al. 2008).

Combination of the laboratory and MSM/Ms (MSM) strains could promote efficient and effective genetic mapping of the anxiety-like behaviors or the behavioral stress responses. MSM is one of the inbred mouse strains derived from Japanese wild mice. Although many researchers have been used laboratory mouse strains to study the genetic mechanisms of behaviors, whose genetic and phenotypic diversities were often limited because most of the laboratory mouse strains are mainly derived from small populations of *Mus musculus domesticus* (Silver LM 1995, Beck JA et al. 2000). One of the ways to solve this problem is to use another subspecies of mouse such as *M. m. musculus*, *M. m. castaneus*, and *M. m. molossinus*. The MSM strain belongs to *M. m. molossinus* (Moriwaki K et al. 2009) and the mice retain behavioral characteristics of wildness as opposed to the laboratory mice (Koide T et al. 2000, Takahashi A et al. 2006, Goto T et al. 2013). In fact, MSM mice show higher anxiety-like behaviors in the open-field tests than C57BL/6JJcl (B6) mice that are one of the laboratory mouse strains (Takahashi A et al. 2006).

Previously, our group conducted genetic analysis of anxiety-like behaviors using a panel of consomic strains, each of which has one pair of chromosomes derived from MSM in place of the corresponding chromosomes on B6 genetic background (Takahashi A et al. 2008). Each consomic strain is represented as B6-ChrN^{MSM}, where the 'N' indicates the substituted chromosome number. The study revealed that B6-Chr17^{MSM} mice show higher anxiety-like behaviors than B6 mice, in which lower vertical activities, higher pausing behavior, higher

stretching behavior, and lower locomotor activities were observed relative to B6 mice. These results suggest that the behavioral differences observed between B6-Chr17^{MSM} and B6 mice are caused by some of the polymorphisms between B6 and MSM in protein-coding genes, non-coding RNA genes, cis-regulatory regions, or some of the other factors on the chromosome 17. However, actual causal genetic factor of the behaviors remained to be studied.

The aim of the present study is to discover the causal gene related to the high behavioral responses to stress using B6-Chr17^{MSM} mice. I first conducted genetic analyses to reveal a locus related to the high anxiety-like behavior, and found PACAP gene as one of the candidate genes in the mapped locus. Second, I investigated whether the peptide sequences, the expression levels, or the distributions of the PACAP are different between B6 and the congenic mice. Based on a knowledge of the PACAP as a neuroendocrine peptide in hypothalamus, I analyzed stress responses to immobilization (restrained stress) in congenic mice to evaluate association of the high PACAP expression with the high behavioral responses to stress.

2.2. Results

2.2.1. Genetic mapping for anxiety-like behaviors

A panel of sub-consomic strains, which cover whole chromosome 17, was developed by using B6 and B6-Chr17^{MSM} mice (Figure 1). I compared behavioral phenotypes between B6 mice and sub-consomic (C4, C3-6, C5-7, T4o, T4, and T103) mice using open-field test (Figure 2A). As with the behavioral characters of B6-Chr17^{MSM} mice in the previous study (Takahashi A et al. 2008), T103 mice showed significantly lower vertical activities (including leaning and rearing behaviors, except for jumping behavior) than B6 mice (mean ± SEM: 46.3 ± 4.5 vs. 57.2 ± 2.9 events, $P < 0.05$), indicating weak exploratory activities. In addition, T4 and T103 mice showed significantly higher pausing behaviors than B6 mice (mean ± SEM: 14.4 ± 0.5 vs. 7.7 ± 0.9 events, 24.4 ± 0.5 vs. 7.7 ± 0.9 events, $P < 0.05$), accounted some of the

defensive behaviors for a novel environment. These results suggest that an overlapping region derived from MSM strain between T4 and T103 strains, named as T103 locus, is one of the loci responsible for open-field behaviors. The other behavioral parameters were not clearly mapped into a particular genetic locus (data not shown).

Based on the latest mouse genome assembly (NCBI Mouse Build 38, GRCm38.p1), the T103 locus spans about 8.3 Mb segment ranged from D17Mit129 (86,688,972 bp) to the end of chromosome 17 (94,987,271 bp). In this genomic region, 56 annotated genes including 26 protein-coding genes, *Epas1*, *Tmem247*, *Atp6v1e2*, *Rhoq*, *Pigf*, *Cript*, *Socs5*, *Mcfd2*, *Ttc7*, *1700011E24Rik*, *Calm2*, *Epcam*, *Msh2*, *Kcnk12*, *Msh6*, *Fbxo11*, *Foxn2*, *Ppp1r21*, *Ston1*, *Gtf2a1l*, *Lhcgr*, *Fshr*, *Nrxn1*, PACAP (*Adycap1*), *Mettl4,* and *Gm2093*, in addition to 8 non-coding genes, and 22 pseudo genes were reported in a previously study (NCBI Annotation Release 104).

In order to refine the mapped region, additional congenic strains, T103-T116, T116, and T119 were developed from T103 mice. I compared behavioral phenotypes between B6 and these congenic mice in an open field test (Figure 2B). At the same time, I analyzed their behaviors using a battery of the behavioral tests; novel cage test, home cage test, open field test, light dark box test, elevated plus maze test, and light enhanced startle response test (Table 3). Consistent with the behavioral traits of T103 mice, T116 mice showed significantly lower vertical activities (mean ± SEM: 46.0 ± 3.6 vs. 57.9 ± 4.5 events, $P < 0.05$) and higher pausing behaviors (mean ± SEM: 21.3 ± 5.8 vs. 5.1 ± 1.6 events, $P < 0.05$) than B6 mice in the open field tests. Among most of the tests, T116 mice showed significantly lower locomotor activities than B6 mice ($P < 0.05$). There was no clear difference between B6 and T103-T116 mice, or B6 and T119 mice in all of the tests. Thus, the MSM-derived regions overwrapped between T103 and T116 strains excluding the region of T119 strain, named as T116-T119 locus, was mapped (Figure 3A).

I successfully mapped a genetic locus responsible for open-field behaviors into T116-T119 locus spanning about 2.6 Mb segment ranged from D17NigT116 (91,588,000 bp) to D17Nig119 (94,190,165 bp) of chromosome 17. In this genomic region, 8 genes with annotation were found in a previous study (Figure 3C and Table 4), of which PACAP gene has solely been reported as protein-coding and functional gene except for seven other pseudo genes (NCBI Annotation Release 104). PACAP gene codes a neuropeptide, pituitary adenylate cyclase activating polypeptide, which acts as a master integrator of stress signaling (Stroth N et al. 2011). Previous studies demonstrated that PACAP knockout mice showed lower anxiety-like behaviors compared to genetic background mice (Hashimoto H et al. 2001), while local injection of PACAP into the hypothalamus induced high anxiety-like behaviors in mice (Norrholm SD et al. 2005). The current results as well as these previous reports suggest that the MSM-derived PACAP gene causes high anxiety-like behaviors in T4, T103, and T116 mice.

2.2.2. Genetic differences of PACAP gene between B6 and MSM strains

There are two possibilities for how genetic differences in PACAP gene cause the behavioral changes. One of the possibilities is polymorphisms in the coding sequence that lead to altered protein products, and the other is polymorphisms in the non-coding sequences that change the expression levels or the spatial localization of the products. Therefore, I evaluated whether the protein function or the expression of PACAP is altered in T103 and T116 mice. In order to compare the PACAP coding sequences between B6 and T103 strains, I determined nucleotide sequences of the PACAP gene by DNA sequencing using PACAP cDNA clones obtained from hypothalamus of B6 and T103 mice. I found that there is no polymorphism in the PACAP coding sequence between B6 and T103 strains. This result means that the PACAP protein function of MSM strain is identical with that of B6 strain.

Although there was no functional difference in the PACAP coding sequences between B6 and

MSM strains, I found some polymorphisms in promoters, 5' untranslated regions (UTRs), and 3' UTRs of the PACAP genes (Table 5). These polymorphisms may affect PACAP mRNA expression levels because it has been demonstrated that a 5'-flanking sequence including the promoter and the 5' UTR of the PACAP gene has functional luciferase activity in a reporter assay (Yamamoto K et al. 1998) and a 3' UTR is generally known to be important to regulate mRNA stability (Harakall SA et al. 1998).

2.2.3. Increased PACAP expression levels in T103 and T116 mice

If change of PACAP expression in central nervous system (CNS) is a cause of the high anxiety-like behaviors in T103 and T116 mice, PACAP mRNA levels should be higher in T103 and T116 than B6 mice. To compare the PACAP mRNA levels in brain between B6, T103, T103-T116, and T116 mice, I measured relative PACAP mRNA levels between strains by quantitative real-time PCR using total RNA samples extracted from whole brains. I found that the PACAP mRNA levels were significantly higher in T103 (mean ± SEM: 1.33 ± 0.05 vs. 1.00 ± 0.05, $P < 0.001$) and T116 (mean ± SEM: 1.20 ± 0.02 vs. 1.00 ± 0.05, $P < 0.001$) compared to B6 mice (Figure 4A). There was no clear difference between B6 and T103-T116 mice (mean ± SEM: 0.95 ± 0.06 vs. 1.00 ± 0.05). These results indicate that the PACAP mRNA levels depend on their genotypes. In order to specify a particular brain region expressing the PACAP mRNA higher than the other genotypes, I measured relative PACAP mRNA levels between strains by quantitative real-time PCR using total RNA samples extracted from each brain region, which were dissected into three anatomical parts, midbrain, hindbrain, and hypothalamus, and spinal cord. In the hypothalamus, the PACAP mRNA levels were significantly higher (mean ± SEM: 1.49 ± 0.15 vs. 1.00 ± 0.05, $P < 0.001$) in T103 than B6 mice (Figure 4B). On the other hand, there was no strain difference in the PACAP mRNA levels in midbrain (mean ± SEM: 1.16 ± 0.12 vs. 1.00 ± 0.09), hindbrain (mean ± SEM:

1.01 ± 0.12 vs. 1.00 ± 0.13), and also spinal cord (mean ± SEM: 1.07 ± 0.11 vs. 1.00 ± 0.09). In the CNS, PACAP mRNA is mainly expressed in hypothalamus (Jens Hannibal, 2002), thus it is likely that differences of the PACAP mRNA levels in the whole brain are mostly attributable to the hypothalamus.

It is assumed that the change of PACAP expression lead to a change in not only PACAP mRNA levels, but also PACAP protein levels. Based on this point, to compare the PACAP protein levels between B6 and T116 mice, I measured the PACAP contents in hypothalamus, in which PACAP-38 is a predominant form (Arimura A et a., 1991), by radioimmunoassay using soluble proteins extracted from the hypothalamus. In the basal condition, the PACAP contents were significantly higher (mean ± SEM: 8.26 ± 0.15 vs. 7.31 ± 0.26 pg/ng protein, $P < 0.005$) in T116 than B6 mice in the hypothalamus (Figure 4C). Together with the results from quantitative real-time PCR, I concluded that PACAP expression levels are high in hypothalamus of T103 and T116 mice.

2.2.4. No difference in spatial distribution of PACAP in T103 and B6 mice

In order to confirm PACAP distributions in hypothalamus of B6 and T103 mice, I detected the PACAP by immunohistochemistry. Because PACAP is strongly localized in the paraventricular nucleus (PVN, Figure 5A) and suprachiasmatic nucleus (SCN, Figure 5B) in hypothalamus, I compared the distribution pattern of the PACAP in those regions. There was no clear difference in the PACAP distribution between B6 and T103 mice. These results indicate that the behavioral differences between B6 and T103 mice are not attributable to the difference of the PACAP distribution.

2.2.5. Validation of PACAP gene involvement

Characterization of phenotypic effects on behaviors of PACAP alleles is important to evaluate an involvement of PACAP gene on the behaviors. Thus I compared allele effects among three

alleles, $PACAP^{B6}$ (B), $PACAP^{MSM}$ (M), and $PACAP^{KO}$ (K). The PACAP knockout allele was developed by homologous recombination using gene-targeting vector in 129/Ola mouse-derived E14tg2a embryonic stem cells (Hashimoto et al. 2001). I made crosses between F1 mice of B6 x T116 and F1 mice of B6 x B6-$PACAP^{KO}$ to make combinations among the alleles. As a result of the cross, four genotypes were obtained, namely B/B, B/K, B/M, and M/M genotypes. The progenies, each of which has one of the four different genotypes, were subjected to an open-field test (Figure 6A). Pausing behaviors were higher in B/M (mean ± SEM: 13.7 ± 1.8 vs. 7.2 ± 1.7 events, $P < 0.05$) and M/M (mean ± SEM: 16.8 ± 3.5 vs. 7.2 ± 1.7 events, $P < 0.01$) than B/B genotypes. There was no significant difference in pausing behaviors between B/M and M/M genotypes (mean ± SEM: 13.7 ± 1.8 vs. 16.8 ± 3.5 events), but the pausing behaviors of M/M genotypes were slightly higher than that of B/M genotypes. B/K genotypes showed similar behavioral phenotypes with B/B genotypes (mean ± SEM: 8.5 ± 2.4 vs. 7.2 ± 1.7 events). I did not observe any significant difference of vertical activities among genotypes.

To confirm the PACAP expression levels in hypothalamus of each PACAP genotype, I measured PACAP mRNA levels by quantitative real-time PCR (Figure 6B). Consistent with the pausing behaviors, B/M (mean ± SEM: 1.52 ± 0.16 vs. 1.00 ± 0.05, $P < 0.001$) and M/M (mean ± SEM: 1.61 ± 0.18 vs. 1.00 ± 0.05, $P < 0.001$) genotypes showed significantly higher PACAP mRNA levels than B/B genotypes. The presences of K allele decreased the PACAP mRNA levels by about half of that of B/B genotypes. These reductions were also observed in M/K genotypes, although the degrees were seemed to be smaller than the case of B/M genotypes.

2.2.6. Prolonged stress responses in T116 mice

PACAP acts as regulator of stress response in HPA axis, and downstream signal of the HPA

axis induces secretion of corticosterone into circulating blood (Agarwal A et al. 2005). If PACAP release into hypothalamus is higher in T116 than B6 mice, it will lead to excess secretion of the corticosterone following an activation of the HPA axis in response to stress in T116 mice. To evaluate this prediction, I measured serum corticosterone levels in B6 and T116 mice at 0, 20, and 60 min start from a restrained stress, and 30, 60, and 120 min following the 60 min stress (Figure 7A). In the basal condition, the serum corticosterone levels were not significantly difference between B6 and T116 mice (mean ± SEM: 47.6 ± 18.4 vs. 45.3 ± 14.3 ng/mL). During the restraints for 60 min, elevated serum corticosterone levels were observed in B6 and T116 mice, but no strain difference was found. After releasing from the stress, the serum corticosterone levels were gradually decreased in both mice, but T116 mice showed slightly higher serum corticosterone levels than B6 mice 120 min after the stress (mean ± SEM: 246.7 ± 18.5 vs. 178.5 ± 28.9 ng/mL).

In addition, I measured serum corticosterone levels in B6 and T116 mice at 6 hour start from a restrained stress, and 2 hour following the tress (Figure 7B). After termination of the 6 hour stress, B6 and T116 mice showed similar serum corticosterone levels with 1 hour start from the stress (mean ± SEM: 415.3 ± 7.9 vs. 397.9 ± 19.2 ng/mL), suggesting that these elevated serum corticosterone levels were supposed to be at a maximal plateau with 1 hour restraint. Next I measured the serum corticosterone levels after 1 hour of the restraint for 6 hour. T116 mice showed significantly higher serum corticosterone levels than B6 mice (mean ± SEM: 133.2 ± 28.3 vs. 29.3 ± 4.1 ng/mL, $P < 0.005$). These results suggest the presence of some of the genetic mechanisms that induce prolonged stress responses in the HPA axis, such as high expression levels of the PACAP gene.

Because it is reported that chronic stress increases PACAP mRNA levels in mouse brain (Hammack SE et al. 2009), I measured PACAP contents in hypothalamus by radioimmunoassay

using mice exposed to restraint stress for 6 hours (Figure 7C). The PACAP contents were significantly higher in T116 than B6 mice (mean ± SEM: 8.13 ± 0.14 vs. 7.37 ± 0.22 pg/ng protein, $P < 0.05$), although their PACAP levels not changed from basal condition (Figure 4C). In other words, T116 mice maintained the higher PACAP levels than B6 mice even after the restraint stress.

I then analyzed behavioral effects of the stress by open-field test immediately following the restraint for 6 hours using B6 and T116 mice (Figure 7D). T116 mice showed significantly lower vertical activities than B6 mice (mean ± SEM: 13.4 ± 3.1 vs. 27.7 ± 5.4 events, $P < 0.05$). Pausing behaviors were not observed in this test situation, whereas wet dog shake behaviors (paroxysmal shudder of entire body reminiscent of a wet dog) were appeared, which were significantly higher in T116 than B6 mice (mean ± SEM: 21.3 ± 1.6 vs. 9.8 ± 2.2 events, $P < 0.05$). In both mice, face washing and grooming behaviors were clearly increased from the basal condition, but there was no significant difference between the strains.

2.3. Discussion

2.3.1. Genetics

In the present study, I mapped an anxiety-related QTL using B6-Chr17^{MSM} consomic mice into T116-T119 locus. Previously, an anxiety-related QTL has been mapped using B6-Chr17$^{A/J}$ consomic mice, in which A/J is one of the classical laboratory strains, in a region between D17Mit39 (74,282,202 bp) and D17Mit221 (90,087,705 bp) on chromosome 17 (Singer JB et al. 2005). As shown in Figure 3A, these two QTLs are not overwrapped. To examine a reason of discrepancy of the QTLs between these two studies, I compared genomic sequences of A/J and MSM strains to that of B6 strain. As with most of the genomic regions, the T116-T119 locus has higher level of genetic polymorphisms between B6 and MSM, than that between B6 and A/J (Figure 3B). Notably, there is no detectable SNP around the PACAP gene locus between B6 and

A/J strains. This result supports that a causal gene of the anxiety-related QTL in A/J is not the PACAP gene, but the other gene located between D17Mit39 and D17Mit221. This is a reason why the PACAP gene was not found as a candidate of the anxiety-related QTL in the previous study.

I found that the PACAP is a strong candidate gene for behavioral responses to stress higher in B6-Chr17^{MSM} mice than B6. However, I still need to do further analyses to examine this finding, because there are still possibilities of involvement of the other non-coding genetic factors in the mapped region. For example, it has been reported that some of the long non-coding RNAs play a role for regulating neural development to mediate behavioral process (Mercer TR et al. 2008, Ponjavic J et al. 2009, Soshnev AA et al. 2011). In addition, spontaneous insertion of a nucleotide sequence is known to cause a phenotypic change such as a case of *fgf4* retrogene, which causes short-legged phenotype in dogs (Parker HG et al. 2009). These possibilities imply a need to evaluate a causal relationship between the behavioral changes and the PACAP gene using reverse genetic approaches such as transgenic or knockout/knockin analyses. In the present study, I conducted a quantitative complementation test to show association of anxiety-like behaviors with PACAP gene using PACAP knockout mice in a method similar to previously studies (Long AD et al. 1996, De Luca M et al. 2003, Yalcin B et al. 2004). Although the results showed high pausing behaviors in homozygote of MSM allele, the other combinations of alleles including the knockout allele did not show any significant phenotypic difference between the alleles. The results suggest that slight increase or decrease in the PACAP expression has no effect on anxiety-like behaviors on B6 genetic background as reported previously (Hashimoto H et al. 2001). To evaluate this observation systematically, I should analyze phenotypic effects of gradual increase in the PACAP expression. Recently, I generated lines of transgenic mouse that express additional copies of the MSM-type PACAP gene, using TolII system (Sumiyama K et al. 2010). I

am currently conducting behavioral and molecular analyses on these transgenic mice.

CRISPR/Cas9 (Clustered Regularly Interspaced Short Palindromic Repeat/ CRISPR associated 9) system is also useful to show the causal relationship between phenotype and gene. This system achieves custom genomic modification, in which a short guide RNA is used to target the Cas9 endonuclease to a genomic region of interest and the Cas9 endonuclease achieve sequence-specific DNA cleavage in the site (Jinek M et al. 2012, Barrangou R et al. 2007). Although the PACAP is a strong candidate gene, actual causal polymorphism in the PACAP gene is still unknown. That's why it is difficult to target a certain nucleotide sequence of the PACAP gene to modify a genomic sequence using the CRISPR/Cas9 system. Molecular analyses of the PACAP expression are necessary to proceed with further research.

2.3.2. PACAP and stress responses

Behavioral responses to stress are often referred to as "fight-or-flight response" that was first described by Walter B. Cannon. This response is also known as fight, flight, or freeze responses, where the freeze response is one of the autonomic responses and frequently observed in small animals such as rodents and birds. In the present study, I observed high pausing behaviors in T103 and T116 mice whose PACAP expression levels are high, during the first 3 min of behavioral observation period in open-field tests. This type of immobility is characteristic to wild mice (Griebel G et al. 1998; Blanchard DC et al. 2001, Takahashi A et al. 2006), and also observed in PACAP-administrated rats (Agarwal A et al. 2005). These facts together with my findings suggest that the PACAP may be involved in stress-dependent immobility responses.

It has been reported that PACAP is widely distributed in CNS, but also expressed in peripheral organs such as retina, pancreas, gonad, and adrenal gland (Miyata A et al. 2000, Cummings KJ et al. 2002). In SAM axis, PACAP signal activates synthesis and secretion of the stress hormones in adrenal gland (Stroth N and Eiden LE 2010). Thus, there is a possibility that

the behavioral responses to stress are directly induced by PACAP in peripheral tissues rather than in hypothalamus. If this is the case, an interpretation of the results will become more complex. In either case, PACAP gene is a strong candidate for the high behavioral responses to stress, although this issue still needs to be examined carefully.

Previous studies showed that several lines of PACAP knockout mouse exhibit lower stress response than wild-type mice (Stroth N and Eiden LE 2010, Tsukiyama N et al. 2011). Based on these reports, I also examined corticosterone levels in T116 mice after restraint stress administration. Although the corticosterone levels of T116 mice were not different from that of B6 mice after 6 h from onset of the stress, it was significantly higher in T116 mice after 2h from the end of the stress administration. The results suggest that corticosterone secretion was elevated up to the maximum level in both strains and an activity for feedback regulation of HPA axis was low in T116 mice than B6. However, it is not clear whether corticosterone secretion is really maximal or not at that time. This question needs to be examined by another experiment such as an exogenous ACTH administration.

PACAP has been implicated as a factor that activates CRH expression in hypothalamus (Agarwal A et al. 2005, Stroth N and Eiden LE 2010). CRH is a main regulator of the stress responses in HPA axis (Aguilera G et al. 2007). In the present study, T116 mice showed higher PACAP expression in hypothalamus and higher corticosterone levels after restraint stress than that of B6 mice. Thus, it was expected that CRH expression is higher in T116 mice than B6 mice. However, I did not find any difference in expression of CRH in hypothalamus at basal condition between T116 and B6 mice (data not shown). These results suggest either possibilities that the neurons with high PACAP expression project to the other neurons or the high PACAP content in neurons is only responsible for stress. In fact, hypothalamic CRH mRNA in PACAP-deficient mice is similar to that of wild-type mice at basal condition, and the levels differed after restraint

stress (Stroth N and Eiden LE 2010). Therefore, it is possible that T116 mice have difference in CRH expression after restraint stress. This possibility is also needed to be investigated further.

PVN and bed nucleus stria terminal (BNST) have been shown to mediate stress responses of HPA axis (Herman JP et al. 2005). Importantly, chronic stress has been shown to increase PACAP expression in these brain regions, and this increase has been proposed to mediate the behavioral responses to stress (Hammack SE et al. 2009). In the present study, PACAP expression in hypothalamus was higher in T103 and T116 than B6 mice, suggesting that the high PACAP expression may be localized in around the PVN or the BNST. PACAP-containing neurons in these brain regions are known to project one another (Kozicz T et al. 2000, Das M et al. 2007). In addition, PACAP is proposed to play as an autocrine/paracrine role within the PVN (Grinevich V et al. 1997). However, a certain pathway by which the high PACAP expression induces prolonged stress responses of the HPA axis in T103 and T116 mice remains to be studied in more detail.

In the present study, I showed possible relationship between the high behavioral responses to stress and the high hypothalamic PACAP expression in adult mice. However, the data do not rule out a possibility that the high PACAP expression affect the formation of CNS through developmental stage. PACAP has a role as a neurotrophic factor in central and peripheral nervous systems (Botia B et al. 2007, Ravni A et al. 2006, DiCicco-Bloom E et al. 2000). Moreover, PACAP during early developmental period influences behaviors in adult mice (Ishihama T et al. 2010). However, I still support the possibility that the high PACAP expression in adult itself play as the cause of the high behavioral responses to stress, given that the previous report showed that intra-PVN infusion of PACAP induce stress response (Huang W et al. 1996, Norrholm SD et al. 2005).

Genetic association studies of PACAP and its receptor genes have been implicated in several

neuropsychiatric diseases such as schizopherenia (Hashimoto R et al. 2007), post-traumatic stress disorder (PTSD) (Ressler KJ et al. 2011), and autistic spectrum disorders (Nijmeijer JS et al. 2010). Importantly, some of these diseases are associated with high expression of the PACAP or the receptors. For example, PACAP blood levels and expression levels of the receptor, PAC1, were high in PTSD patients (Ressler KJ et al. 2011). In other cases, a copy number of PACAP receptor, *VIPR2*, was associated with schizopherenia, in which 7q36.3 chromosomal region is duplicated or triplicated (Levinson DF et al 2011, Vacic V et al. 2011). Therefore, transgenic mouse overexpressing the PACAP or the receptor genes was proposed to be useful to address an implication of PACAP signaling in psychiatric conditions (Shen S et al. 2013). Thus, the PACAP overexpressing T116 mice will provide a useful animal model for studying these psychiatric disorders. In particular, T116 mice showed prolonged hormonal responses to stress. The hormonal responses to stress are known to be exaggerated in PTSD patients (Elzinga BM et al. 2003, Liberzon L et al. 1999), and the prolonged corticosterone treatment in early life increase the corticosterone response to stress in adulthood (Pravosudov VV and Kitaysky AS 2006, Spencer et al. 2009). These data suggest that the importance in the negative feedback regulation of the HPA axis. Taken together, an understanding of the mechanisms by which the high PACAP expression causes high behavioral and hormonal responses to stress in T116 mice may promote better understanding of the pathological mechanisms of the disorders and facilitate a development of effective therapeutic drugs to treat the diseases.

The present study investigated whether the PACAP expression is changed in T116 mice relative to B6 mice. I observed high PACAP expression in hypothalamus of T116 mice. There are several polymorphisms in PACAP gene between B6 and MSM strain, suggested that one or more of these polymorphisms is a cause of the high PACAP expression. In the Part II of this article, I examined that what molecular mechanisms are associated with the high PACAP

expression.

2.4. Conclusion

The present findings provide a strong candidate PACAP gene for the previous study in witch B6-Chr17^{MSM} consomic strain exhibits higher behavioral responses to stress than B6. PACAP overexpressing T116 mice showed behavioral and hormonal responses to stress recapitulating several observations from the PACAP-deficient or the PACAP-administrated animals. Together with the previous genetic studies that revealed an association of PACAP gene with psychiatric disorders, I suggest that T116 mice provide a useful animal model for understanding the physiological mechanisms underlying stress-induced activation of the HPA axis. Future studies using restrained mice will provide further insight into the pathological effects of the high PACAP expression in regulating stress responses of the HPA axis.

2.5. Materials and methods

2.5.1. Animals

MSM was established at the National Institute of Genetics (NIG) (Mishima, Japan) and B6 was purchased from CLEA Japan, Inc (Tokyo, Japan). B6-Chr17^{MSM} was established by substituting one pair of chromosome 17 of B6 with that of MSM on genetic background of B6 (Takada T et al. 2008). B6-PACAP^{KO} mice were kindly provided by Dr. Hashimoto (Hashimoto H et al. 2001). The animals were bred in standard sized plastic cages on wood chips at the NIG. B6 male mice (9-14 weeks of age) were used in this study and compared to age-matched test animals. The animals were maintained under standard environmental conditions (12-h light/dark cycle, light from 6:00 to 18:00; temperature-controlled room, 23±2 ^{o}C). Food and water were available *ad labium*. The animals were weaned around from 25 days to 31 days of age and housed in same sex groups. The animals were maintained according to NIG guidelines, and all experimental protocols were approved by the Institutional Animal Care and Use Committee at

the NIG.

2.5.2. Establishment of sub-consomic and congenic strains

F1 progeny, which were made by crossing B6 female mice with B6-17^{MSM} male mice, were backcrossed to B6, and the offspring that carried desirable recombination within chromosome 17 were used for the subsequent cross. Those individuals were backcrossed to B6 one more time to obtain the cohort with same recombined segment of MSM chromosome. They were then intercrossed to make homozygotes for the substituted segment. A panel of congenic strains established in this study is listed in Figure 1

2.5.3. Genotyping of the markers in chromosome 17

Sequences and genomic location of primer sets used for genotyping are showed in Table 1 and Figure 1.

2.5.4. Behavioral test

2.5.4.1. Open-field test

The open-field tests were performed as descried previously (Takahashi A et al. 2008). The open-field was composed of a floor space of 60 cm x 60 cm and with walls height of 40 cm. The floor and the walls were constructed of white polyvinylchloride plastic board. The arena was illuminated with two lamps placed 90 cm above the arena. The light level was 365 lux at the center of the arena. The open-field was surrounded by black curtains except for the front side. I observed the animal's behaviors at the front of the open-field directly. The area and the motion of the animals were captured by a video camera placed over its center.

Animals were brought in a dimly lit place of the test room at least 1 hour before the start of the first test on the day to minimize the effects of transfer. At the start of each test, the arena was cleaned up with 70 % ethanol and paper towels. The wet floor and the walls were air-dried with a fan. Each animal was gently picked up by its tail with tweezers and placed on the same corner of

the open-field. During the ten-minute trial, their behaviors were observed directly. For counting the behavioral events, I made a software system, tanaMove ver0.01 Goto T et al. 2013). Following 13 kinds of behaviors were counted; Activity, stretching, leaning, rearing, grooming, face-washing, jumping, pausing, freezing, and wet dog shake. The activities were analyzed using a video tracking system (Image OF, O'hara & Co. Ltd., Japan). Vertical activities were obtained as a sum of the leaning and the rearing. At the end of each test, the number of defecations and presence of urination were also counted. All the tests were carried out during the light period (13:00-18:00).

2.5.4.2. Elevated plus maze

The elevated plus maze tests were performed as descried previously (Takahashi A et al. 2008). The elevated plus maze composed of two open arms with low edge (30 x 5 x 0.25 cm) and two closed arms enclosed by clear acrylic plastic wall (30 x 5 x 15 cm) that extended from a central platform (5 x 5 cm). Each arm was floored in white acrylic board. The apparatus was elevated 60 cm above the floor. The apparatus was dimly lit (150 lux).

Animals were brought in a dimly lit place of the test room at least 1 hour before the start of the first test on the day to minimize the effects of transfer. At the start of each test, the arena was cleaned up with 70 % ethanol and paper towels. The wet floor and the walls were air-dried with a fan. Each animal was gently picked up by its tail with tweezers and placed on the central platform. During the ten-minute trial, their behaviors were counted as follows. Activity (cm), number of entries into the open-arm or closed-arm, and duration in the open-arm or closed arm were analyzed using a video tracking system (Image EPM; O'hara & Co. Ltd., Japan). At the end of each test, the number of defecations and presence of urination were also counted. All the tests were carried out during the light period (13:00-18:00).

2.5.4.3. Acoustic and light-enhanced startle response test

Test sessions began by placing the mouse in a clear Plexiglas holding cylinder placed on a piezoelectric accelerometer, which detected the vibrations caused by startle reflection to the sound of the mouse by using SR-LAB system (San Diego Instruments, USA). A 65 dB background noise was presented throughout the test session. Briefly, animal was acclimated for 2 min and then it was presented with startle trials (120 dB, 40 ms sound pulse) and startle trials (30 ms 95, 105 or 120 dB sound).

2.5.5. Cloning and sequence of PACAP gene

Mouse PACAP cDNA was amplified by the RT-PCR from the total RNAs which were isolated from the hypothalamus of B6 and T103 mice. A set of primers corresponding to the beginning and the end of coding region of mouse PACAP cDNA were used for PCR (Table 2). The amplified DNA fragments were ligated into the pGEM-T Easy vector (Promega, France) and then sequenced using Prism BigDye Terminator version 3.1 Cycle Sequencing Kit (Applied Biosystems, Germany).

2.5.6. RNA isolation, reverse transcription, and real-time quantitative PCR

Five males in each strain were used to quantify mRNA levels. All samples were collected between 14:00 and 18:00. The animals were sacrificed by cervical dislocation and decapitated, and then brains were removed from the skull, and quickly dissected into three parts, hypothalamus, midbrain, and hindbrain. The hypothalamus was dissected as a complex of thalamus and hypothalamus in this study. In addition, pituitary gland, spinal cord, and both sides of adrenal glands were isolated. Each tissues were homogenized in Trizol regent (15596-026, Life Technologies, Japan), and the total RNAs were isolated from the homogenates according to manufacturer’s protocol followed by DNA digestions with TURBO DNA-free DNase (AM1907, Life Technologies, Japan). First-strand cDNA was synthesized with PrimeScript II 1st strand cDNA Synthesis Kit (6210A, TaKaRa, Japan) in accordance with manufacturer’s instructions,

using 2 ug of total RNAs and oligo dT primer. Real-time quantitative PCR was carried out with SYBR Premix Ex Taq II (Tli RNaseH Plus) (RR820S, TaKaRa, Japan) on a Thermal Cycler Dice® Real Time System II (TP900, TaKaRa, Japan). Gene-specific primers (see Table 2) were designed by using Primer3 (Rozen and Skaletsky, 2000; http://frodo.wi.mit.edu/). The primers were validated by using Reverse e-PCR (Rotmistrovsky K et al. 2004, http://www.ncbi.nlm.nih.gov/tools/epcr/), and checked mismatching on MSM genome or transcripts by using MSM genome database (http://molossinus.lab.nig.ac.jp/msmdb/). The mRNA levels were measured in duplicate for each sample. All data were normalized to β-actin mRNA levels.

2.5.7. Protein extraction and radioimmunoassay

PACAP-38 contents were measured by radioimmunoassay using hypothalamic region of mouse brains. For sampling hypothalamic tissues, mice were anesthetized and decapitated. The brains were removed from the skull, and immediately followed by dissection of a block containing the hypothalamic region. Hypothalamic peptides were extracted as described previously (Beinfeld MC and Korchak DM 1985). Briefly, hypothalamic blocks were homogenized in 250 ul of boiling water at 100 ^{o}C for 10 min, centrifuged at 7500 rpm for 35min at 4 ^{o}C and the supernatants were transferred into new tubes. The pellets were re-extracted by homogenization with 250 ul of 0.5 M acetic acid at room temperature followed by centrifugation. The combined supernatants were centrifuged again and the supernatants were transferred into new tubes, stored at -80 ^{o}C until radioimmunoassay. Total protein contents in supernatants were measured in triplicate for each sample (BCA protein assay kit; Pierce, Rockford, IL). Radioimmunoassays were performed using ^{125}I RIA kit (RK-052-05; Phoenix Pharmaceuticals Inc., Belmont, CA, USA) according to manufacturer's suggested protocol. Briefly, PACAP-38 concentrations were analyzed using extracts containing 12.5 ug of protein in each sample and

quantified in triplicate according to a standard curve using known PACAP-38 concentrations (10-1280 pg/reaction).

2.5.8. Sectioning and immunohistochemistory

Animals were deeply anesthetized with Somnopentyl (0.01 ml/g weight, i.p., Kyoritsu Seiyaku Co., Japan) and transcardially perfused with Stefanini's fixative (2 % paraformaldehyde, 0.2 % picric acid in PBS, pH 7.2). The brains were then removed and postfixed in the same fixative for 1 hour, cryoprotected in 10% sucrose in PBS for 6 hours, 20 % sucrose in PBS for 6 hours and 30 % sucrose in PBS for 6 hours at 4 ^{o}C. Afterwards, they were frozen in Optimal Cutting Temperature (Sakura Finetechnical Co., Japan) compound, and stored at -80 ^{o}C until use. Frozen samples were sectioned with a cryostat at 50 um thickness and mounted on MSA-coated glass slides (Matsunami Glass Co., Japan). For the immunohistochemical visualization, the ABC-method was carried out according to the instructions of the ABC Elite Kit (Vector Labs., USA) with Vector DAB Substrate Kit (Vector Labs., USA). Briefly, sections were treated with 0.3 % hydrogen peroxide for 20 min, incubated in the 3 % normal horse serum in PBS for 1 hour at room temperature and then incubated in PACAP-38 rabbit primary antiserum (Y041, Yanaihara Institute Inc., Japan; diluted 1:2000 in PBS) diluted in the 1 % normal horse serum in PBS for 1 hour in room temperature. After the washing in PBS three times, sections were incubated in horse anti-rabbit IgG (Vector Labs., USA, diluted 1:200 in PBS) for 1 hour at room temperature. The sections were then washed three times in PBS and incubated in avidin-biotin-peroxidase complex (diluted 1:200 in PBS). Finally, sections were visualized with DAB containing 0.06 % nickel ammonium sulfate.

2.5.9. Restrained stress

A dozen of animals in each strain was used in this experiment. Each animal was placed in individual home cage approximately 18 hours before the restrained stress. All experiments were

started between 9:00 and 10:30 AM. Animals were separated into two groups: six untreated mice (non-stressed controls) and six treated mice (restrained continuously for 6 hours). Each animal in treated group was placed in a 50 ml Falcon Tube (BD Biosciences Cell Culture, Japan), which was cut a hole at the bottom of tube to allow the animal to breath by facing to the hole during restraining, and placed in the home cage during the restraining treatment. After six hours' treatment, each mouse was euthanized with CO_2 immediately to remove a brain sample.

2.5.10. Serum sampling and ELISA assay for corticosterone

Blood samples were taken from the heart within 3 minutes after anesthesia with CO_2 and were allowed to clot at room temperature for approximately 1 hour. The clots were removed by centrifugation (15 min at 3,000$\times g$), the supernatants were collected and stored at -80 ^{o}C until assayed. Corticosterone levels were measured by ELISA assay (YK240, Yanaihara, Japan) according to the manufacturer's instructions.

2.5.11. Statistical analysis

Statistical significance was determined by analysis of variance (ANOVA) followed by post hoc comparison using the Dunn's Method for multiple-comparison of behavioral data and Tukey-Kramer's Method for gene expression data. Differences were considered to be significant at $P < 0.05$. The calculations were performed using StatView 5.0 (SAS Institute Inc., USA).

2.6. References

Agarwal A et al. (2005). Pituitary adenylate cyclase-activating polypeptide (PACAP) mimics neuroendocrine and behavioral manifestations of stress: Evidence for PKA-mediated expression of the corticotropin-releasing hormone (CRH) gene. Brain Res Mol Brain Res. 138: 45-57.

Aguilera G et al. (2007). Negative regulation of corticotropin releasing factor expression and limitation of stress response. Stress. 10: 153-161.

Arimura A et al. (1991). Tissue distribution of PACAP as determined by RIA: highly abundant in the rat brain and testes. Endocrinology. 129(5): 2787-9.

Badr FM et al. (1960). Genetic variation in adrenal weight: strain differences in the development of the adrenal glands of mice. Acta Endocrinol (Copenh). 58(2): 191-201.

Bailey JS, Grabowski-Boase L, Steffy BM, Wiltshire T, Churchill GA et al. (2008) Identification of quantitative trait loci for locomotor activation and anxiety using closely-related inbred strains. Genes Brain Behav. 7(7):761-9.

Bakshi VP and Kalin NH (2002). Animal models and endophenotypes of anxiety and stress disorders In: Davis KL, Charney DS, Coyle JT, Nemeroff CB (eds). Neuropsychopharmacology: The Fifth Generation of Progress. Lippincott Williams & Wilkins: Philadelphia, PA. pp 883-900.

Barnett SA (1958). Exploratory behavior. Br J Psychol. 49: 289-310.

Barnett SA (1963). The Rat: a Study in Behaviour. Aldine Publishing Co, Chicago.
Barnett SA and Cowan PE (1976). 1976. Activity, exploration, curiosity and fear: An ethological study. Interdisc Sci Rev. 1: 43-62.
Barrangou R et al. (2007). CRISPR provides acquired resistance against viruses in prokaryotes. Science. 315(5819): 1709-12.
Beck JA et al. (2000). Genealogies of mouse inbred strains. Nat Genet.24(1): 23-5.
Beinfeld MC and Korchak DM (1985). The regional distribution and the chemical, chromatographic, and immunologic characterization of motilin brain peptides: the evidence for a difference between brain and intestinal motilin-immunoreactive peptides. J Neurosci. 5(9): 2502-9.
Blanchard RJ et al. (1998). Defensive behaviors in wild and laboratory (Swiss) mice: the mouse defense test battery. Physiol Behav. 65: 201-209.
Blanchard DC et al. (2001). Mouse defensive behaviors: pharmacological and behavioral assays for anxiety and panic. Neurosci Biobehav Rev. 25(3): 205-18.
Botia B et al. (2007). Neurotrophic effects of PACAP in the cerebellar cortex. Peptides. 28(9): 1746-52.
Calhoun JB (1962). The ecology and sociology of the norway rat. Bethesda: US Department of Health, Education, and Welfare pp.1-288.
Cummings KJ et al. (2002). Mouse pituitary adenylate cyclase-activating polypeptide (PACAP): gene, expression and novel splicing. Mol Cell Endocrinol. 192(1-2): 133-45.
Das M et al. (2007). Hypothalamic and brainstem sources of pituitary adenylate cyclase-activating polypeptide nerve fibers innervating the hypothalamic paraventricular nucleus in the rat. J Comp Neurol.500(4): 761-76.
De Luca M et al. (2003). Dopa decarboxylase (Ddc) affects variation in Drosophila longevity. Nat Genet. 34(4): 429-33.
DiCicco-Bloom E et al. (2000). Autocrine expression and ontogenetic functions of the PACAP ligand/receptor system during sympathetic development. Dev Biol. 219(2): 197-213.
Dunn TB and Andervont HB (1963). Histology of neoplasms and non-neoplastic lesions found in wild mice maintained under laboratory conditions. J Natl Cancer Inst. 31: 873-901.
Elzinga BM et al. (2003). Higher cortisol levels following exposure to traumatic reminders in abuse-related PTSD. Neuropsychopharmacology. 28(9): 1656-65.
Frazer KA et al. (2007) A sequence-based variation map of 8.27 million SNPs in inbred mouse strains. Nature. 448(7157):1050-3.
Goto T et al. (2013). Selection for reluctance to avoid humans during the domestication of mice. Genes Brain Behav. 12(8): 760-70.
Griebel G et al. (1998). Genetic differences in the mouse defense test battery. Aggressive Behav. 23(1): 19-31.
Grinevich V et al. (1997). Effects of pituitary adenylate cyclase-activating polypeptide (PACAP) on corticotropin-releasing hormone (CRH) gene expression in the rat hypothalamic paraventricular nucleus. Brain Res. 773(1-2): 190-6.
Hall CS (1934) Emotional behavior in the rat. I. Defecation and urination as measures of individual differences in emotionality. J. comp. Psychol. 18(3):385-403.
Hall CS (1936a) Emotional behavior in the rat. II. The relationship between need and emotionality. J. comp. Psychol. 22(1):61-68.
Hall CS (1936b) Emotional behavior in the rat. III. The relationship between emotionality and ambulatory activity. J. comp. Psychol. 22(3):345-352.
Hall CS and Ballachey EL (1932). A study of the rat's behaviour in a field: a contribution to methods in comparative psychology. Univ Calif Publ Psychol. 6: 1-12.
Hammack SE et al. (2009). Chronic stress increases pituitary adenylate cyclase-activating peptide (PACAP) and brain-derived neurotrophic factor (BDNF) mRNA expression in the bed nucleus of the stria terminalis (BNST): roles for PACAP in anxiety-like behavior. Psychoneuroendocrinology. 34(6): 833-43.
Hannibal J (2002). Pituitary adenylate cyclase-activating peptide in the rat central nervous system: An immunohistochemical and in situ hybridization study. J Comp Neurol. 453(4): 389-417.
Harakall SA et al. (1998). Induction of multiple pituitary adenylate cyclase activating polypeptide (PACAP) transcripts through alternative cleavage and polyadenylation of proPACAP precursor mRNA. Ann N Y Acad Sci. 865: 367-74.
Hashimoto H et al. (2001) Altered psychomotor behaviors in mice lacking pituitary adenylate cyclase-activating polypeptide (PACAP). Proc Natl Acad Sci U S A. 98(23):13355-60.
Hashimoto R et al. (2007). Pituitary adenylate cyclase-activating polypeptide is associated with schizophrenia. Mol Psychiatry. 12(11): 1026-32.
Herman JP and Cullinan WE (1997). Neurocircuitry of stress: central control of the hypothalamo-pituitary-adrenocortical axis. Trends Neurosci. 20(2): 78-84.
Herman JP et al. (2005). Limbic system mechanisms of stress regulation: hypothalamo-pituitary-adrenocortical axis. Prog Neuropsychopharmacol Biol Psychiatry. 29(8): 1201-13.

Ishihama T et al. (2010). Environmental factors during early developmental period influence psychobehavioral abnormalities in adult PACAP-deficient mice. Behav Brain Res. 209(2): 274-80.
Ising M and Holsboer F (2006). Genetics of stress response and stress-related disorders. Dialogues Clin Neurosci. 8(4): 433-44.
Jinek M et al. (2012). A programmable dual-RNA-guided DNA endonuclease in adaptive bacterial immunity. Science. 337(6096): 816-21.
Kerbusch JML et al. (1981). Behavioral responses to novelty in mice: A reanalysis. Behav Genet. 11: 373-377.
Koide T et al. (2000). Multi-phenotype behavioral characterization of inbred strains derived from wild stocks of Mus musculus. Mamm Genome. 11(8): 664-70.
Kozicz T et al. (1998). The source of origin of PACAP- and VIP-immunoreactive fibers in the laterodorsal division of the bed nucleus of the stria terminalis in the rat. Brain Res. 810(1-2): 211-9.
Levinson DF et al. (2011). Copy number variants in schizophrenia: confirmation of five previous findings and new evidence for 3q29 microdeletions and VIPR2 duplications. Am J Psychiatry. 168(3): 302-16.
Liberzon I et al. (1999). Neuroendocrine and psychophysiologic responses in PTSD: a symptom provocation study. Neuropsychopharmacology. 21(1): 40-50.
Long AD et al. (1996). Genetic interactions between naturally occurring alleles at quantitative trait loci and mutant alleles at candidate loci affecting bristle number in Drosophila melanogaster. Genetics. 144(4): 1497-510.
Makara GB et al. (2004). The role of vasopressin in hypothalamo-pituitary-adrenal axis activation during stress: an assessment of the evidence. Ann N Y Acad Sci. 1018: 151-61.
Makino J et al. (1991). Temporal structure of open-field behavior in inbred strains of mice. Jpn Psychol Res. 33: 145-152.
Mercer TR et al. (2008). Specific expression of long noncoding RNAs in the mouse brain. Proc Natl Acad Sci U S A.105(2): 716-21.
Miller BH et al. (2010). Phenotypic Characterization of a Genetically Diverse Panel of Mice for Behavioral Despair and Anxiety. PLoS One. 5(12): e14458.
Miller RA et al. (2000) Mouse (Mus musculus) stocks derived from tropical islands: new models for genetic analysis of life-history traits. J. Zool., 250, 95-104.
Miyata A et al. (2000). Genomic organization and chromosomal localization of the mouse pituitary adenylate cyclase activating polypeptide (PACAP) gene. Ann N Y Acad Sci. 921: 344-8.
Moriwaki K et al. (2009). Unique inbred strain MSM/Ms established from the Japanese wild mouse. Exp Anim. 58(2): 123-34.
Nijmeijer JS et al. (2010). Identifying loci for the overlap between attention-deficit/hyperactivity disorder and autism spectrum disorder using a genome-wide QTL linkage approach. J Am Acad Child Adolesc Psychiatry. 49(7): 675-85.
Norrholm SD, Das M, Legradi G (2005) Behavioral effects of local microinfusion of pituitary adenylate cyclase activating polypeptide (PACAP) into the paraventricular nucleus of the hypothalamus (PVN). Regul Pept. 128(1):33-41.
Parker HG et al. (2009). Science. An expressed fgf4 retrogene is associated with breed-defining chondrodysplasia in domestic dogs. 325(5943): 995-8.
Ponjavic J et al. (2009). Genomic and transcriptional co-localization of protein-coding and long non-coding RNA pairs in the developing brain. PLoS Genet. 5(8): e1000617.
Pravosudov VV and Kitaysky AS. (2006). Effects of nutritional restrictions during post-hatching development on adrenocortical function in western scrub-jays (Aphelocoma californica). Gen Comp Endocrinol. 145(1): 25-31.
Ravni A et al. (2006). The neurotrophic effects of PACAP in PC12 cells: control by multiple transduction pathways. J Neurochem. 98(2): 321-9.
Ressler KJ et al. (2011). Post-traumatic stress disorder is associated with PACAP and the PAC1 receptor. Nature. 470(7335): 492-7.
Rotmistrovsky K et al. (2004). A web server for performing electronic PCR. Nucleic Acids Res. 32 (Web Server issue): W108-12.
Rozen S and Skaletsky H (2000). Primer3 on the WWW for general users and for biologist programmers. Methods Mol Biol. 132: 365-386.
Schatzberg AF et al. (2014). HPA axis genetic variation, cortisol and psychosis in major depression. Mol Psychiatry. 19(2): 220-7.
Shen S et al. (2013). PACAP and PAC1 receptor in brain development and behavior. Neuropeptides. 47(6): 421-30.
Sherwood NM et al. (2000). The origin and function of the pituitary adenylate cyclase-activating polypeptide (PACAP)/glucagon superfamily. Endocr Rev. 21(6): 619-70.
Silver LM (1995). Mouse Genetics. Oxford Univ. Press, New York
Singer JB et al. (2005) Mapping Quantitative Trait Loci for Anxiety in Chromosome Substitution Strains of Mice.
Smith SM and Vale WW (2006). The role of the hypothalamic-pituitary-adrenal axis in neuroendocrine responses to stress. Dialogues Clin Neurosci. 8(4): 383-95.

Soshnev AA et al. (2011). A conserved long noncoding RNA affects sleep behavior in Drosophila. Genetics. 189(2): 455-68.
Spencer KA et al. (2009). Postnatal stress in birds: a novel model of glucocorticoid programming of the hypothalamic-pituitary-adrenal axis. Endocrinology. 150(4): 1931-4.
Steimer T (2011). Animal models of anxiety disorders in rats and mice: some conceptual issues. Dialogues Clin Neurosci. 13(4): 495-506.
Stroth N and Eiden LE (2010). Stress hormone synthesis in mouse hypothalamus and adrenal gland triggered by restraint is dependent on pituitary adenylate cyclase-activating polypeptide signaling. Neuroscience. 165(4): 1025-30.
Stroth N et al. (2011). PACAP: a master regulator of neuroendocrine stress circuits and the cellular stress response. Ann N Y Acad Sci. 1220: 49-59
Sumiyama K et al. (2010). A simple and highly efficient transgenesis method in mice with the Tol2 transposon system and cytoplasmic microinjection. Genomics. 95(5): 306-11.
Takada T et al. (2008). Mouse inter-subspecific consomic strains for genetic dissection of quantitative complex traits. Genome Res. 18(3): 500-8.
Takahashi A et al. (2006). Multivariate analysis of temporal descriptions of open-field behavior in wild-derived mouse strains. Behav Genet. 36(5): 763-74.
Takahashi A et al. (2008). Systematic analysis of emotionality in consomic mouse strains established from C57BL/6J and wild-derived MSM/Ms. Genes Brain Behav. 7(8): 849-58.
Tokuda M (1935). An eighteenth century Japanese guide-book on mouse-breeding. J Hered. 26: 481-484.
Trut LN (1999) Early Canid Domestication:The Farm-Fox Experiment. American Scientist. 87(2): 160-169.
Tsukiyama N et al. (2011). PACAP centrally mediates emotional stress-induced corticosterone responses in mice. Stress. 14(4): 368-75.
Ulrich-Lai YM and Herman JP (2009). Neural regulation of endocrine and autonomic stress responses. Nat Rev Neurosci. 10(6): 397-409.
Vacic V et al. (2011). Duplications of the neuropeptide receptor gene VIPR2 confer significant risk for schizophrenia. Nature. 471(7339): 499-503.
Yalcin B et al. (2004). Genetic dissection of a behavioral quantitative trait locus shows that Rgs2 modulates anxiety in mice. Nat Genet. 36(11): 1197-202.
Zhou Z et al. (2008). Genetic variation in human NPY expression affects stress response and emotion. Nature. 452(7190): 997-1001.

3. Part II: Molecular relationship between PACAP expression and TG repeat polymorphism

3.1. Introduction

PACAP is a pleiotropic neuropeptide that has roles of hypophysiotropic hormone, neurotransmitter, neurotrophic factor, neuromodulator, and neuroprotector (Vaudry D et al. 2000, Vaudry D et al. 2009). Among abundant knowledge about the functions, PACAP has been reported for many implications of stress response physiology. PACAP is highly abundant in hypothalamus and has been shown to not only activate the HPA axis, but also to increase the synthesis of several stress hormones (Hashimoto H et al. 2011). PACAP distributed in PVN is thought to act as an excitatory neuropeptide that lead to behavioral responses to stress (Agarwal A et al. 2005, Norrholm SD et al. 2005). Neuroanatomical mechanisms for regulating the behavioral responses to stress via PACAP have not been fully understood yet. However, fragmented information of PACAP function has been reported on the neuroanatomical mechanisms. PACAP knockout mice displayed remarkable changes in anxiety-like behaviors such as hyperactive and explosive jumping behaviors in an open field (Hashimoto H et al. 2001). These mice showed not only abnormal psychomotor behaviors, but also physiological changes in which activities of the HPA and the SAM axes, and also synthesis of stress hormones were decreased (Hamelink C et al. 2002, Stroth N and Eiden LE 2010). Furthermore, chronic stress increases PACAP expression in BNST and its signaling mediates anxiety-like behavioral responses to the stress (Hammack SE et al. 2009). Collectively, these evidences suggest that neuroendocrine system controlling the anxiety-like behaviors depends on a regulation of the PACAP expression.

PACAP was first isolated from ovine hypothalamus as a stimulator of adenylate cyclase in rat anterior pituitary cells (Miyata A et al. 1989). There are two different C-terminally amidated forms in PACAP isoforms, 38 (PACAP-38,

HSDGIFTDSYSRYRKQMAVKKYLAAVLGKRYKQRVKNK) and 27 (PACAP-27, HSDGIFTDSYSRYRKQMAVKKYLAAVL) amino acids. PACAP27 is a truncated form of PACAP38 sharing the first 27 amino acids (Miyata A et al. 1990, Lie M et al. 1998, Lie M et al. 1999). In nervous tissues, predominant form of PACAP is the PACAP38 whose concentration is higher from 10 to 50-fold than that of the PACAP27 (Hannibal J et al. 1995). PACAP cDNAs have been cloned from several species and its amino acid sequences were highly conserved in vertebrate (Montero M et al. 2000, Vaudry D et al. 2000, Vaudry D et al. 2009). PACAP gene, which is also called as *acetylate cyclase activating polypeptide 1* (*Adcyap1*) gene, encodes a precursor protein that contains a signal peptide, a cryptic peptide, a PACAP-related peptide (PRP), and a PACAP38. Although the PRP has similar functions to the PACAP in non-mammalian vertebrates, the functions of PRP seem to be lost in mammals (Tam JK et al. 2007). Expressions of the PACAP have been detected in many tissues including brain, gonad, testis, ovary, adrenal gland, pancreas, thymus, and eye (Miyata A et al. 2000, Cummings KJ et al. 2002). In the CNS, the PACAP is distributed in a various cell bodies and nerve fibers in neuronal cells (Hannibal J 2002).

Regulation mechanism of the PACAP expression has been addressed mainly in rodent and human (Ohkubo S et al. 1994, Yamamoto K et al. 1998, Hahsimoto H et al. 2000, Cummings KJ et al. 2002, Fukuchi M et al. 2004, Sugawara H et al. 2004, Harakall SA et al. 1998, Kim MS et al. 2002, Tominaga A et al. 2008). Upstream region of mouse PACAP gene contains several transcriptional regulatory elements such as a cAMP response element (CRE) (Deutsch et al 1988), a 12-O-tetradecanoylphorbol-13-acetate response element (TRE) (Angle et al. 1987), neural-restrictive silencer-like elements (NRSLE1 and NRSLE2) (Sugawara H et al. 2004), a growth hormone factor-1 (GHF-1) binding site (Bodner et al. 1988), and a thyroid transcription factor-1 (TTF-1) binding site (Kim MS et al. 2002).

As described in the part I, I assumed that the high PACAP expression levels in T103 and T116 mice are caused by genetic polymorphisms between B6 and MSM strains, in which some of molecular mechanisms such as a gene regulation mediated by transcription factors, and a post-transcriptional regulation including splicing and DNA/RNA structure will be involved. MSM strain has many polymorphisms in the PACAP gene compared with reference genome sequence of B6 strain, in which there are 28 polymorphisms among exons and introns (Table 5 and Figure 8A). I searched sequence motifs on the polymorphic sites that could act as a transcriptional regulatory element in either B6 or MSM strain, and then discovered several putative elements around a transcription start sites (TSSs) of the PACAP gene. One of the putative elements that modulate PACAP expression was a microsatellite at the DNA segment, Chr 17, D17Mit123 locus in an intronic region of the PACAP gene (Dietrich WF et al. 1994, Hudson TJ et al. 2001).

The microsatellite (TG dinucleotide repeat) at the D17Mit123 locus is highly polymorphic site. This microsatellite has been widely used for genetic mapping as a marker at the end of chromosome 17, and itself has been become a representative example of microsatellite instability in tumor in mice (Wong E et al. 2002, van Oers JM et al. 2013). The TG repeat is located in a intronic region of the PACAP gene. As suggested in previous study (Yamamoto K et al. 1998), the TG repeat might have a role of regulatory element of the PACAP gene because a TG repeat at an upstream region generally affects gene expression (Rich A et al. 1984, Hamada H et al. 1984, Li YC et al. 2004). Some of the TG repeats have an enhancer-like activity through the adoption of a left-handed DNA conformation (Z-DNA) (Haniford DB and Pulleyblank DE 1983, Nordheim A and Rich A 1983), which is susceptible to a single-stranded endonuclease (Hamada H et al. 1984, Weintraub H 1983). However, no experimental evidence has yet been reported on the regulation of the PACAP gene via the TG repeat sequence.

The TG repeat might have a role of regulator of a RNA splicing efficiency of the PACAP exon 1B because some of the dinucleotide repeats including TG repeat can regulate a splicing efficiencies of an adjacent exon (Hui J et al. 2005, Hui J and Bindereif A 2005). One of mechanisms underlying the regulation of splicing efficiency is that the splicing efficiency depends on a thermodynamic stability of a RNA secondary structure (Hefferon TW et al. 2004). The stability increases as a length of the TG repeat. Moreover, some of the TG repeats have been implicated in an alternative splicing via TG dinucleotide binding proteins such as a heterogeneous nuclear ribonucleoprotein L (hnRNP L) and a trans-activation response element (TAR) DNA-binding protein 43 (TDP-43) (Hung LH et al. 2008, Buratti E and Baralle FE 2001). These proteins function as an activator or a repressor of splicing whose actions depend on locations and lengths of the TG repeat.

Here I attempted to clarify an involvement of the TG repeat polymorphisms in PACAP expressions. Correlations of the PACAP expressions and lengths of the TG repeats were evaluated using several mouse strains. I analyzed a potential regulator depended on the length of TG repeat in the PACAP gene as an enhancer-like element of a gene expression and a regulator-like element of an alternative splicing. I provide evidences for the high PACAP expression implicating in an alternative splicing of 5' UTRs. Implications of the TG repeat in the above molecular mechanisms were validated using a luciferase reporter assay.

3.2. Results

3.2.1. PACAP transcript expressions associated with the lengths of TG repeat in several mouse strains

The TG repeat is located in a second intron adjacent to a second exon of the PACAP gene (Figure 8A). A distance between the TG repeat and the second exon, named as 1B, is only 24 bp. To investigate a genetic diversity of the TG repeat, I determined nucleotide sequences of TG

repeats in available mouse strains including 25 laboratory strains and 13 wild-derived strains (Table 6). All of the analyzed laboratory strains exhibit short TG repeat lengths ranged from 26 to 38 TG dinucleotides, while most of the analyzed wild-derived strains exhibit long TG repeat lengths ranged from 36 to 53 TG dinucleotides, except for AVZ strain.

In order to evaluate a relationship between PACAP expression levels and the lengths of the TG repeats, I compared PACAP mRNA levels by quantitative real-time PCR using total RNAs isolated from hypothalamus of several mouse strains, whose TG repeat lengths vary from 26 to 53 TG dinucleotides (Figure 8B). Results in HMI mice were excluded from further analysis given that the enhancer-like activities of TG repeat will decrease when the repeat length is longer than 50 (Hamada H et al. 1984). The comparison showed a positive correlation between the lengths of the TG repeat and the PACAP mRNA levels ($y = 0.099x – 0.57$, Pearson's correlation coefficient $R^2 = 0.27$, $P = 0.0004$). The PACAP mRNA levels peaked in 41 TG dinucleotides in BFM mice. In addition, the PACAP mRNA levels of laboratory mice were clearly lower than wild-derived mice. These results suggest that an enhancer-like activity depend on the lengths of TG repeat described above.

I next examined whether the PACAP gene splicing depends on the lengths of the TG repeats. I compared PACAP transcripts by reverse-transcript PCR using the total RNAs isolated from hypothalamus in mice of a number of strains whose lengths of the TG repeats are vary from 26 to 53 dinucleotides (Figure 8C). The PACAP transcripts were analyzed using a specific primer set that designed to amplify the exons from 1A to 5. In each mouse, three types of the PACAP transcripts, named as splice variant 1, 2, and 3, were observed in an agarose-gel electrophoresis. Among the PACAP transcripts, expression levels of the splice variant 3 were clearly higher in the wild-derived mice than the laboratory mice, except for CHD mice. I determined nucleotide sequences and structures of each PACAP transcript in B6 mice by DNA sequencing using cDNA

clones of the PACAP transcripts (Figure 8D). In the results, I found that the PACAP transcripts have alternate 5' UTR sequences with coding sequences identical to each other. Although the cDNA sequence of the PACAP splice variant 1 was found in databases such as AceView (http://www.ncbi.nlm.nih.gov/IEB/Research/Acembly/), its functional details were still unknown. It was assumed that the PACAP splice variant 1 is an immature mRNA that has to go through a splicing process before it can be translated because the sequence still contains an intronic sequence. The PACAP splice variant 2 and 3 are identical to the PACAP cDNAs reported in previous study (Yamamoto K et al. 1998). Notably, the PACAP splice variant 3 is identical to the first published PACAP cDNA (Okazaki K et al. 1995). A major structural difference between these PACAP splicing variants was existence of the exon 1B that is excluded in the PACAP splicing variant 3. These results indicate that longer lengths of the TG repeat result in higher expression of the PACAP splice variant 3. In other words, the length of TG repeat may affect the RNA splicing of the PACAP gene via a role of regulator-like element of splicing of the exon 1B.

Based on a knowledge about splicing efficiency depends on thermodynamic stability of RNA secondary structure (Hefferon TW et al. 2004), I assumed that thermodynamic stability of RNA secondary structure of the UG repeat of PACAP gene is higher in MSM than B6. To elucidate this idea, I predicted the thermostability by mfold 3.4 (Mathews DH et al. 1999, Zuker M et al. 2003) (http://mfold.rna.albany.edu/?q=mfold/) (Figure 8E). $(UG)_{40}$ dinucleotide repeat in MSM (dG = -20.3 Kcal/mol) showed higher thermostability than $(UG)_{26}$ dinucleotide repeat in B6 (dG = -10.6 Kcal/mol). This result supports my assumption that the TG repeat has a role of regulator-like element of splicing.

3.2.2. Analyses of the PACAP transcript expressions in T103 mice

To uncover detailed difference of the PACAP expression between strains, I need to analyze the PACAP expression at the transcript levels using mouse strains that have polymorphisms in

PACAP gene on the same genetic background. To be certain that I compared the PACAP transcripts by Northern blotting using Poly(A)$^+$ mRNAs in hypothalamus between B6 and T103 mice and DIG-labeled mouse PACAP cDNA probe (Figure 9A). The patterns of PACAP signals of T103 mice seemed to be similar to that of B6 mice. However, there is a limitation in quantitative comparison of relative abundances of particular PACAP transcripts in this method because it was difficult to distinguish the various PACAP transcripts from its mixture. In addition, alternate polyadenylation site in the 3' UTR of PACAP gene would also related in this matter (Harakall SA et al. 1998). Therefore, instead of Northern blotting, I compared the PACAP transcripts by reverse-transcription PCR using the samples of B6 and T103 mice with the primer set designed to amplify the PACAP transcripts from exon 1A to exon 5 (Figure 9B). In both mice, PACAP splice variant 1, 2, and 3 were observed in the agarose-gel electrophoresis. Among the PACAP transcripts, splice variant 3 were clearly higher in T103 than B6 mice. To determine whether all or parts of the PACAP transcripts were highly expressed in hypothalamus of T103 mice, I examined the PACAP transcript expressions by quantitative real-time PCR using total RNAs isolated from hypothalamus of B6 and T103 mice with the specific primer sets corresponding to each of the PACAP transcripts (Figure 9C). The PACAP splice variant 3 mRNA levels were significantly higher in T103 than B6 mice (mean ± SEM: 2.05 ± 0.20 vs. 1.00 ± 0.13, $P < 0.005$), while the PACAP splice variant 1 and 2 mRNA levels were similar levels between T103 and B6 mice (mean ± SEM: 1.29 ± 0.13 vs. 1.00 ± 0.09). In addition, I calculated the ratios of the PACAP splice variant 3 to the PACAP splice variant 1 and 2 in order to normalize the mRNA levels with total mRNA levels of the PACAP transcripts (Figure 9D). The ratio of the PACAP splice variant 3 to the PACAP splice variant 1 and 2 were significantly higher in T103 than B6 mice (mean ± SEM: 1.59 ± 0.08 vs. 1.00 ± 0.09, $P < 0.005$). These results suggest that the RNA splicing of the PACAP exon 1B is affected by some

molecular mechanisms via genetic differences between B6 and T103 mice.

Next I examined whether the RNA splicing of the PACAP exon 1B is also changed in other brain regions of T103 mice. I compared the ratios of the PACAP splice variant 3 to the PACAP splice variant 1 and 2 by quantitative real-time PCR using the total RNAs isolated from midbrain, hindbrain, and spinal cord between B6 and T103 mice (Figure 9D). Similar to the results in hypothalamus, the ratios of the PACAP splice variant 3 to the PACAP splice variant 1 and 2 were also significantly higher in other brain regions of T103 than B6 mice ($P < 0.005$). These results indicate that regulation of the RNA splicing of the PACAP exon 1B does not depend on the tissue-specific mechanisms such as gene regulation mediated by tissue-specific transcription factor. It means that there is another molecular mechanism independent to up-regulation of the PACAP gene expression.

3.2.3. PACAP minigene replicates *in vivo* expression associated with length of the TG repeat

To examine activities of the TG repeat as enhancer-like and splicing regulator-like elements *in vivo*, I constructed two types of PACAP minigene, pTG26 and pTG40 (Figure 10A). The pTG26 minigene contained a 2.2 kb 5'-flanking region of the PACAP gene derived from B6 genome, exon 1A, exon 1B, and portion of exon 2, with intronic sequences flanking each exon, fused in-frame to a *Gaussia* luciferase (GLuc) reporter cDNA through a self-cleaving viral sequence (P2A) sequence in expression vector. This minigene was designed to mimic the PACAP expression machinery *in vitro*. The GLuc reporter is naturally secreted into the extracellular medium via the endoplasmic reticulum (ER) and the Golgi complex (Inouye et al. 1992). This reporter is useful for dual reporter assay with *Cypridina* Luciferase (CLuc) reporter (Tannous BA et al. 2005, Goerke AR et al. 2008). The CLuc reporter is also naturally secreted protein via the similar mechanisms with GLuc reporter. The PACAP-GLuc fusion gene was linked through a

P2A sequence because the signal peptide of the PACAP gene will lead undesired effects on secretion of the GLuc reporter (Ibrahimi A et al. 2009, de Felipe P and Ryan MD 2004). The pTG40 construct was developed by replacing the $(TG)_{26}$ dinucleotide repeat sequence in pTG26 construct with a $(TG)_{40}$ dinucleotide repeat sequence derived from MSM genome. These minigenes were transfected into PC12 cells by nucleofection with control pTK-CLuc vectors for normalization of the GLuc activities. The pTK-CLuc vector contains a CLuc gene driven by a herpes simplex virus thymidine kinase (TK) promoter. I measured the luciferase activities by dual luciferase reporter assays using the supernatants obtained from the transfected cells (Figure 10B). The luciferase activity of the pTG26 minigene was significantly lower than that of pTG40 minigene (mean ± SEM: 1.50 ± 0.01 vs. 1.00 ± 0.03, $P < 0.0001$). To compare the expression levels of the PACAP-GLuc fusion gene between the pTG26 and the pTG40 minigenes, I measured the PACAP-GLuc fusion mRNA levels by quantitative real-time PCR using the total RNAs isolated from the transfected PC12 cells (Figure 10C). The PACAP-GLuc fusion mRNA levels were significantly higher in pTG40 than pTG26 minigenes (mean ± SEM: 2.55 ± 0.25 vs. 1.00 ± 0.16, $P < 0.005$).

Next I examined the splicing regulator-like activity of the TG repeat. I compared the PACAP-GLuc fusion transcripts by reverse-transcript PCR using the total RNAs isolated from cells transfected with pTG26 and pTG40 minigenes (Figure 10D). Three PACAP-GLuc fusion transcripts, named as splice variant T1, T2, and T3, were observed (Figure 10E). These transcripts consist of fusion sequences of the alternate 5' UTRs derived from the PACAP gene and the GLuc gene. The PACAP-GLuc fusion splice variant T3 were significantly higher in pTG40 than pTG26 minigenes (mean ± SEM: 1.27 ± 0.03 vs. 1.00 ± 0.05, $P < 0.005$) (Figure 10F). These expression differences were comprehensively confirmed by quantitative real-time PCR using the samples with specific primer sets corresponding to each PACAP-GLuc

fusion transcript (Figure 10G). The ratios of the PACAP-GLuc fusion splice variant T3 to the PACAP-GLuc fusion splice variant T1 and T2 were significantly higher in pTG40 than pTG26 minigenes (mean ± SEM: 1.67 ± 0.10 vs. 1.00 ± 0.05, $P < 0.001$). These results are consistent with observations made in minigenes of cystic fibrosis transmembrane conductance regulator (*CFTR*) gene (Hefferon TW et al. 2004), where RNA splicing of exon 9 depends on TG repeat number. Hence, I concluded that the TG repeat length can affect the RNA splicing of the PACAP gene *in vivo* and *in vitro*.

3.2.4. Comparison of translation efficiencies between the PACAP transcripts

My next objective was to reveal functional difference of the PACAP transcripts. I searched the uORFs in the PACAP transcripts by ORF Finder (http://www.bioinformatics.org/sms2/orf_find.html) using cDNA sequences of the PACAP transcripts (Figure 11A). I found two types of uORFs, named as uORF1 and uORF2, in the 5' UTRs of the PACAP splice variants. The both uORFs are located in the different reading frames (out-of-frame) compared to the main ORF with no overlap. The uORF1 is common among the PACAP splice variants and the uORF2 is found in the PACAP splice variant 1 and 2. Because the uORFs may reduce the translation efficiencies of the PACAP splice variants, these results suggest that the PACAP splice variant 3 has higher translation efficiency than the others.

The uAUG sequence is known to be favored by some specific sequence (GCC)GCC(A or G)CCATGG, which is called as kozak consensus sequence (Kozak M 1987). Kozak sequence is not essential for gene expression, but it has strong effects on the translation efficiency in vertebrates. It was reported that the A or G at position −3 is critical for the translation efficiency. In the alternative splicing of PACAP transcripts, the uAUG contexts was switched by inclusion or skipping of the PACAP exon 1B (Figure 11B). This switching will lead changes in the translation efficiencies between the PACAP splice variants because A at position −3 in the

PACAP splice variant 3 might have higher translation efficiency than C at position −3 in the other splice variants. To evaluate the AUG contexts as translation start site, I compared probabilities of the translation start site of each AUG in the uORFs and the ORFs by NetStart, in which translation start sites were predicted using neural networks (Pedersen AG and Nielsen H 1997) (http://www.cbs.dtu.dk/services/NetStart/) (Table 7). In the PACAP splice variant 1 and 2, the AUGs of the main ORFs showed lower probability scores than that of uORFs. The PACAP splice variant 3 had higher probability score in main ORF than that of uORF, and the value was the highest score among the PACAP splice variants. These results also indicate that the PACAP splice variant 3 has higher translation efficiency than the others.

To compare the translation efficiency of the 5' UTR sequence in the PACAP splice variants *in vitro*, I cloned cDNAs of the PACAP-GLuc fusion splice variants from an agarose-gel electrophoresis and constructed pT1, pT2, and pT3 expression vectors, which express the PACAP-GLuc fusion splice variants under the control of a TK promoter (Figure 12A). I measured the luciferase activities by dual luciferase reporter assays using the supernatants obtained from the PC12 cells transfected with the vectors (Figure 12B). The luciferase activity was the highest in the pT3 expression vector among the expression vectors ($P < 0.0001$). The pT2 expression vector showed higher luciferase activity than the pT1 expression vectors (mean ± SEM: 1.67 ± 0.02 vs. 1.00 ± 0.01, $P < 0.0001$), but lower than the pT3 expression vector (mean ± SEM: 1.67 ± 0.02 vs. 2.40 ± 0.03, $P < 0.0001$). To compare the mRNA expression levels of the expression vectors, I detected the transcripts by reverse-transcript PCR using the total RNAs isolated from the transfected PC12 cells (Figure 12C). Although the luciferase activities were different between the expression vectors, the mRNA levels were not clearly different. From these results, I concluded that the PACAP splice variant 3 has higher translation efficiency than the others.

3.3. Discussion

3.3.1. The regulation of PACAP expression

In the present study, I proposed some molecular mechanisms associated with polymorphisms in PACAP gene by which TG repeat influences PACAP expression as enhance and splicing regulator. However, it is not able to rule out other possibilities for an association of other molecular mechanisms such as transcriptional regulatory elements. In fact, the PACAP expressions were not completely correlated with lengths of the TG repeats in mouse strains. This result suggests another molecular mechanism for the PACAP expression. For example, I found a SNP (rs50376855) between MSM and B6 at 125 bp upstream from the first exon of the PACAP gene that forms a consensus sequence of thyroid transcription factor-1 (TTF-1) binding site, CTGAAG in MSM strain (Bruno MD et al. 1995). Interestingly, the TTF-1 is known to regulate the PACAP expression in hypothalamus of rat (Kim MS et al. 2002, Lee BJ et al. 2001), suggested that the high PACAP expression in hypothalamus may be caused by this SNP rs50376855. To confirm this idea, I need to analyze the promoter activity of the PACAP gene with two types of expression constructs which carry the SNP of B6 or MSM alleles, respectively.

There are several examples that microsatellite polymorphism is associated with quantitative genetic variation of behaviors or disorders. A microsatellite in 5' regulatory region of vasopressin 1a receptor (*v1ar*) gene is associated with the gene expression levels and influence social behaviors in prairie voles (Hammock ET et al. 2005). In human *CFTR* gene, exon 9 is spliced depending on length of TG repeat polymorphism via a mechanism of thermodynamic stability of the RNA secondary structure (Cuppens H et al. 1998). Given that the alternative splicing of exon 9 results in a nonfunctional CFTR protein, excess level of splicing on the exon 9 leads to development of cystic fibrosis (Chu CS et al. 1991, Chu CS et al 1993). It has been reported that GT repeat in first intron of human heme oxygenase-1 (*HO-1*) associates with several

pathological conditions in which the long GT repeat allele is associated with low levels of HO-1 via a regulation of alternative splicing of 5'-UTR exons (Exner M et al. 2004, Kramer M et al. 2013). Most of these findings are associated with gene expression, alternative splicing, and translation efficiency, suggesting that regulation of the PACAP expression via enhancer and splicing regulator-like activities of the TG repeat is a reasonable mechanism for the high PACAP expression in T103 and T116 mice.

PACAP has been reported for possible association with some psychiatric disorders (Hashimoto R et al. 2007, Ressler KJ et al. 2011, Nijmeijer JS et al. 2010). Given that some of the disease-related genes have a microsatellite repeat in the introns, I searched a microsatellite in the human PACAP gene (data not shown). Although the human PACAP gene does not contain TG repeat in the second intron, I found another microsatellite (TA dinucleotide repeat) within the 3'-UTR as reported previously (Pérez-Jurado LA and Francke U 1993). Genetic association between the TA repeat polymorphisms and human diseases was found in patients with hypertension in previous study (Rutherford S et al. 2004). This study indicated that flanking sequence of the microsatellite in the human PACAP gene associates with the hypertension. However, significant impact on risk of the disease was not found for the length of TA repeats. Currently, there is no evidence that a microsatellite in the human PACAP gene influences the gene expression, but my findings provide supportive evidences that simple sequence repeats is one of the sources of some of the psychiatric disorders via quantitative genetic variation as previously proposed (Kashi Y et al. 1997, Kashi Y and King DG 2006, Li YC et al. 2004).

An effective method for demonstrating a relationship between a phenotype of interest and a microsatellite was proposed previously (Huang W et al. 2013). In the study, authors modified a tandem repeat sequence in genome DNA using transcription activator-like effector nucleases (TALEN) system via a double-strand break repairing. The modified genomes showed variable

lengths of the tandem repeat. This method would be useful to examine the causal relationship between the high behavioral responses to stress and the TG repeat polymorphisms in the present study. Given that the modification mechanisms of TALEN system is similar to CRISPR/Cas9 (Clustered Regularly Interspaced Short Palindromic Repeat/ CRISPR associated 9) system (Jinek M et al. 2012, Barrangou R et al. 2007), the tandem repeat modification would be also achieved using CRISPR/Cas9 system. Therefore, CRISPR/Cas9 system provides a quick and reasonable experiment for further studies.

3.3.2. TG repeat polymorphism of PACAP gene in mouse genome

Lengths of the TG repeat in the PACAP gene were clearly separated between laboratory and wild-derived strains, suggesting that the gene might be responsible for behavioral differences between laboratory mice and wild mice, so-called “wildness”. In order to examine this possibility, I conducted *in silico* genome-wide screening for separations of microsatellite repeat lengths between laboratory and wild strains using a database, MMDBJ, for microsatellite polymorphisms in a variety of mouse strains (Sakai T et al. 2004). In the database, genetic information about more than 9,000 loci of simple sequence polymorphisms from 10 laboratory strains, 11 wild-derived strains, and 2 fancy mice derived strains are available. I conducted statistical analyses to detect microsatellites which are significantly different in lengths between two groups, laboratory and wild-derived strains. In the result, 12 intragenic and 15 intergenic microsatellites were significantly ($P < 0.05$, Student’s t-test) separated between laboratory and wild-derived strains (Table 8). As I expected, a microsatellite in D17Mit123 corresponding to the TG repeat in the PACAP gene was ranked at 10th highest position in a list of genes based on the degree of the p-values. The result indicates a significant difference of the TG repeat lengths of the PACAP gene associate with differences between laboratory and wild-derived strains. Most of the other microsatellite lengths were widely dispersed among laboratory and wild-derived strains. These

dispersions of the microsatellite lengths were compatible with a fact that classical laboratory strains had originated from mixed founder population (Wade CM et al. 2002).

Genetic separation of the TG repeat length in the PACAP gene between laboratory and wild-derived strains together with the function as a regulatory element implies an existence of natural selection or artificial selection during domestication on the PACAP gene. Currently, I am interested in a detection of some signatures of selective sweep in the PACAP gene locus by comparing genomic polymorphisms of laboratory and wild mice. Future study will uncover the significance of genetic variation of the PACAP gene in behavioral divergence among mice.

3.4. Conclusion

The current study demonstrated that the TG repeat in the second intron of the PACAP gene regulates the gene regulation via molecular mechanisms such as enhancer and splicing regulators. Evaluation of the translation efficiency of the PACAP transcripts indicated a positive secondary effect of the splicing regulation on the PACAP expression. The TG repeat polymorphisms may act as one of the sources of quantitative phenotypic variation among wild and domesticated mice. Together with the study in the part I, my study demonstrated that molecular mechanisms of the PACAP gene expression via the TG repeat may explain some of the differences of behavioral stress response between B6 and MSM mice.

3.5. Materials and methods

3.5.1. Animals

Follow the methods in Part I.

3.5.2. DNA probe synthesis

Digoxigenin labeled DNA probe were synthesized by PCR using PCR DIG Probe Synthesis Kit (11636090910, Roche, Japan) with Ex-taq polymerase (RR001A, TaKaRa, Japan). A 525 bp protein-coding sequence of PACAP gene was amplified from a PACAP cDNA of T116 mice. A

452 bp sequence of GAPDH gene was amplified from cDNA synthesized from total RNAs of T116 mice. Probes were stored at -80 °C until use.

3.5.3. Poly(A)$^+$ mRNA preparation and Northern blotting

Tissue and total RNA samples were collected as described above. Poly(A)$^+$ mRNA were isolated with *Oligotex™ -dT30<Super>* mRNA Purification Kit（From Total RNA） (9086, TaKaRa, Japan) according to the manufacturer's instructions.

1 ug Poly(A)$^+$ mRNA were denatured at 65 °C for 10 min in loading buffer (25 % (w/v) formamide, 18.5 % (w/v) formaldehyde, 5 % (w/v) glycerol, 1.25 % (w/v) bromophenol blue in MOPS buffer), electroporated at 3 V/cm^2 in MOPS buffer (20 mM MOPS, 5 mM sodium acetate, 2 mM EDTA, pH 7.0) with denaturing gel (1.5 % (w/v) agar, 2 % (w/v) formaldehyde in MOPS buffer), and transferred onto a positively charged Hybond-N$^+$ nylon membrane (RPN82B, GE Healthcare, Japan). RNAs were cross-linked to the membrane with 450 nm UV for 2 min. The membranes were prehybridized at 37 °C for 30 min with DIG Easy Hyb (11603558001, Roche, Japan), and hybridized overnight at 50 °C with DIG-Easy Hyb containing 50 ng/ml denatured DIG-labeled DNA probe (see above). To remove extra probes, membranes were washed thrice with 2.0 x SSC and 0.1 % SDS for 25 min at room temperature, twice with 0.5 x SSC and 0.1 % SDS for 15 min at 50 °C and twice with 0.1 x SSC and 0.1 % SDS for 15 min at 50 °C. To detect the signals, membranes were rinsed for 5 min in maleic acid buffer (0.1 M maleic acid, 0.15 M NaCl, pH 7.5) containing 0.3 % (w/v) Tween 20, blocked for 2 hours in blocking solution (1 % (w/v) blocking reagent in maleic acid buffer), incubated for 30 min in antibody solution (Anti-Digoxigenin-AP, Fab fragments (11093274910, Roche, Japan) diluted 1:10,000 in blocking solution) and washed thrice for 15 min in maleic acid buffer containing 0.3 % (w/v) Tween 20. To visualize the bands, membranes were equilibrated for 5 min in detection buffer (0.1 M Tris-HCl, 0.1 M NaCl, pH 9.5), sealed in plastic Hybri-Bag Hard (S-1001, Cosmo Bio,

Japan) containing CDP-Star, ready-to-use (12041677001, GE Healthcare, Japan), incubated for 5 min and the extra solution was removed. Membranes were exposed at room temperature to Hyperfilm ECL (28-9068-36, GE Healthcare, Japan) in a cassette for up to 3 h depending on the signal strength.

3.5.4. Construction of reporter vectors

In order to make an expression construct, pPACAP-P2A-GLuc (pTG26), pTK-GLuc (NEB, N8084S) was used as backbone vector. The TK promoter sequence upstream of GLuc gene (from -790 to -1) was replaced by PACAP gene sequence containing the promoter and the exons. The PACAP gene sequence (from -2230 to +106) was cloned from genomic DNA extracted from B6 mouse tail as described above. Briefly, the PACAP gene sequence was amplified by PCR using a set of primer pair (Table 2). The PCR product was cloned into the pGEM-T Easy vector. The end of PACAP gene exon 2 was fused with the beginning of GLuc gene through the self-cleaving viral sequence (P2A). The P2A sequence was synthesized as described previously (Abdelilah et al. 2009). Additional pPACAP-P2A-GLuc (pTG40) vector was generated by replacing the AflII-PspXI site of the PACAP gene intron 2 (from -691 to +107) containing dinucleotide $(GT)_{26}$ repeat by corresponding sequence of MSM genome.

To generate pTK-PACAP5UTR-P2A-GLuc (pT1, pT2, and pT3) vectors, PACAP cDNAs were amplified by the RT-PCR from the total RNAs which were isolated from the hypothalamus of T103 mouse. A set of primer pair (Table 2) were used for the PCR amplification. The PCR products were cloned into the pGEM-T Easy vector. The sequence containing a TK promoter, a GLuc gene, and a SV40 poly A in pTK-GLuc vector was sub-cloned into the multi-cloning site in pGEM-T Easy vector, resulting in pGEM-TK-GLuc vector. The sequences containing a 5'-UTR and a exon 2 of the PACAP cDNA (from -880 to +106) were inserted into the beginning of the GLuc gene in pGEM-TK-GLuc vector.

3.5.5. Cell culture

The rat pheochromocytoma PC12 (ATCC) cells were grown on collagen coated 100-mm plastic cull culture dish (Nunc) in Dulbecco's modified Eagle's medium (DMEM) (Sigma) with 10% fetal calf serum and 10% horse serum.

3.5.6. Luciferase assay

3.0 x 10^6 cells were transfected with 5 ug of plasmid DNA by electroporation using Amaxa Nucleofector system II with solution V and Nucleofection program U-029 (Lonza, Walkersville, MD). 0.5 ug of pTK-CLuc vector was co-transfected for normalization of the GLuc activity. Then cells were plated separately in quadruplicate at 3.75 x 10^5 cells/well on poly-L-lysine coated 48-well plates (Nunc). 24 hours after the electroporation, medium supernatants from each well were collected and stored at -80 ^oC until luciferase assay. Luciferase activities were measured by BioLux *Gaussia* Luciferase Flex Assay Kit (NEB, E3308S) and BioLux *Cypridina* Luciferase Assay Kit (NEB, E3309S) according to manufacturer's protocol. The GLuc activities were normalized by the CLuc activities.

3.5.7. RNA extraction from cells

Total cellular RNAs were isolated from the transfected cells with Trizol regent (Invitrogen, Carlsbad, CA) as described above with minor modifications. To remove the proteins completely, samples were phenol chloroform treated twice. To avoid contamination of the plasmid DNA, samples were treated with RNase-free DNase twice.

3.5.8. *In silico* genome-wide screening

Data of microsatellite polymorphisms were obtained from MMDBJ (http://www.shigen.nig.ac.jp/mouse/mmdbj/). Although there were problems of multiple comparisons, I used Student's t-test to conduct rough screening in this study.

3.5.9. Statistical analysis

Statistical significance was determined by analysis of variance (ANOVA) followed by post hoc comparison using the Tukey-Kramer's Method for gene expression data. Differences were considered to be significant at $P < 0.05$. The calculations were performed using StatView 5.0 (SAS Institute Inc., USA).

3.6. References

Agarwal A et al. (2005). Pituitary adenylate cyclase-activating polypeptide (PACAP) mimics neuroendocrine and behavioral manifestations of stress: Evidence for PKA-mediated expression of the corticotropin-releasing hormone (CRH) gene. Brain Res Mol Brain Res. 138(1): 45-57.

Bruno MD et al. (1995). Lung cell-specific expression of the murine surfactant protein A (SP-A) gene is mediated by interactions between the SP-A promoter and thyroid transcription factor-1. J Biol Chem. 270(12): 6531-6.

Buratti E and Baralle FE (2001). Characterization and functional implications of the RNA binding properties of nuclear factor TDP-43, a novel splicing regulator of CFTR exon 9. J Biol Chem. 276(39): 36337-43.

Calvo SE et al. (2009). Upstream open reading frames cause widespread reduction of protein expression and are polymorphic among humans. Proc Nati Acad Sci U S A. 106(18): 7507-12.

Chu CS et al. Genetic basis of variable exon 9 skipping in cystic fibrosis transmembrane conductance regulator mRNA. Nat Genet. 3(2): 151-6.

Chu CS et al. Variable deletion of exon 9 coding sequences in cystic fibrosis transmembrane conductance regulator gene mRNA transcripts in normal bronchial epithelium. EMBO J. 10(6): 1355-63.

Cummings KJ et al. (2002). Mouse pituitary adenylate cyclase-activating polypeptide (PACAP): gene, expression and novel splicing. Mol Cell Endocrinol. 192(1-2): 133-45.

Cuppens H et al. (1998). Polyvariant mutant cystic fibrosis transmembrane conductance regulator genes. The polymorphic (Tg)m locus explains the partial penetrance of the T5 polymorphism as a disease mutation. J Clin Invest. 101(2): 487-96.

Dietrich WF et al. (1994). A genetic map of the mouse with 4,006 simple sequence length polymorphisms. Nat Genet. 7(2 Spec No):220-45.

Exner M et al. (2004). The role of heme oxygenase-1 promoter polymorphisms in human disease. Free Radic Biol Med. 37(8): 1097-104.

Fukuchi M et al. (2004). Activity-dependent transcriptional activation and mRNA stabilization for cumulative expression of pituitary adenylate cyclase-activating polypeptide mRNA controlled by calcium and cAMP signals in neurons. J Biol Chem.279(46): 47856-65.

Goerke AR et al. (2008). Cell-free metabolic engineering promotes high-level production of bioactive Gaussia princeps luciferase. Metab Eng. 10(3-4): 187-200.

Hamada H et al. (1984). Characterization of genomic poly(dT-dG).poly(dC-dA) sequences: structure, organization, and conformation. Mol Cell Biol. 4(12): 2610-21.

Hamada H et al. (2006). Enhanced gene expression by the poly(dT-dG).poly(dC-dA) sequence. Mol Cell Biol. 4(12): 2622-30.

Hamelink C et al. (2002). Pituitary adenylate cyclase-activating polypeptide is a sympathoadrenal neurotransmitter involved in catecholamine regulation and glucohomeostasis. Proc Natl Acad Sci U S A. 99(1): 461-6.

Hammack SE et al. (2009). Chronic stress increases pituitary adenylate cyclase-activating peptide (PACAP) and brain-derived neurotrophic factor (BDNF) mRNA expression in the bed nucleus of the stria terminalis (BNST): roles for PACAP in anxiety-like behavior. Psychoneuroendocrinology. 34(6): 833-43.

Hammock EA et al. (2005). Association of vasopressin 1a receptor levels with a regulatory microsatellite and behavior. Genes Brain Behav. 4(5): 289-301.

Haniford DB and Pulleyblank DE (1983). Facile transition of poly[d(TG) x d(CA)] into a left-handed helix in physiological conditions. Nature. 302(5909): 632-4.

Hannibal J et al. (1995). Gene expression of pituitary adenylate cyclase activating polypeptide (PACAP) in the rat hypothalamus. Regul Pept. 55(2): 133-48.

Hannnibal J (2002). Pituitary adenylate cyclase-activating peptide in the rat central nervous system: an immunohistochemical and in situ hybridization study. J Comp Neurol. 453(4): 389-417.

Harakall SA et al. (1998). Induction of multiple pituitary adenylate cyclase activating polypeptide (PACAP) transcripts through alternative cleavage and polyadenylation of proPACAP precursor mRNA. Ann N Y Acad Sci. 865: 367-74.

Harakall SA et al. (1998). Induction of multiple pituitary adenylate cyclase activating polypeptide (PACAP)

transcripts through alternative cleavage and polyadenylation of proPACAP precursor mRNA. Ann N Y Acad Sci. 865: 367-74.
Hashimoto H et al. (2000). Synergistic induction of pituitary adenylate cyclase-activating polypeptide (PACAP) gene expression by nerve growth factor and PACAP in PC12 cells. J Neurochem. 74(2): 501-7.
Hashimoto H et al. (2001). Altered psychomotor behaviors in mice lacking pituitary adenylate cyclase-activating polypeptide (PACAP). Proc Natl Acad Sci U S A. 98(23): 13355-60.
Hashimoto H et al. (2011). PACAP is implicated in the stress axes. Curr Pharm Des. 17(10): 985-9.
Hashimoto R et al. (2007). Pituitary adenylate cyclase-activating polypeptide is associated with schizophrenia. Mol Psychiatry. 12(11): 1026-32.
Hefferon TW et al. (2004). A variable dinucleotide repeat in the CFTR gene contributes to phenotype diversity by forming RNA secondary structures that alter splicing. Proc Natl Acad Sci U S A. 101(10): 3504-9.
Huang W et al. (2013). Tandem repeat modification during double-strand break repair induced by an engineered TAL effector nuclease in zebrafish genome. PLoS One. 8(12): e84176.
Hudson TJ et al. (2001). A radiation hybrid map of mouse genes. Nat Genet. 29(2): 201-5.
Hui J and Bindereif A (2005). Alternative pre-mRNA splicing in the human system: unexpected role of repetitive sequences as regulatory elements. Biol Chem. 386(12): 1265-71.
Hui J et al. (2005). Intronic CA-repeat and CA-rich elements: a new class of regulators of mammalian alternative splicing. EMBO J. 24(11): 1988-98.
Hung LH et al. (2008). Diverse roles of hnRNP L in mammalian mRNA processing: a combined microarray and RNAi analysis. RNA. 14(2): 284-96.
Ibrahimi A et al. (2009). Highly efficient multicistronic lentiviral vectors with peptide 2A sequences. Hum Gene Ther. 20(8): 845-60.
Inouye, S et al. 1992. Imaging of luciferase secretion from transformed Chinese hamster ovary cells. Proc. Natl. Acad. Sci. 89: 9584-7.
Kashi Y and King DG (2006). Simple sequence repeats as advantageous mutators in evolution. Trends Genet. 22(5): 253-9.
Kashi Y et al. (1997). Simple sequence repeats as a source of quantitative genetic variation. Trends Genet. 13(2): 74-8.
Kim MS et al. (2002). Regulation of pituitary adenylate cyclase-activating polypeptide gene transcription by TTF-1, a homeodomain-containing transcription factor. J Biol Chem. 277(39): 36863-71. Epub 2002 Jul 16.
Kozak M (1986). Point mutations define a sequence flanking the AUG initiator codon that modulates translation by eukaryotic ribosomes. Cell. 44(2): 283-92.
Kozak M (1987). An analysis of 5'-noncoding sequences from 699 vertebrate messenger RNAs. Nucleic Acids Res. 15(20): 8125-48.
Kozak M (1987). At least six nucleotides preceding the AUG initiator codon enhance translation in mammalian cells. J Mol Biol. 196(4): 947-50.
Kramer M et al. (2013). Alternative 5' untranslated regions are involved in expression regulation of human heme oxygenase-1. PLoS One. 8(10): e77224.
Lee BJ et al. (2001). TTF-1, a homeodomain gene required for diencephalic morphogenesis, is postnatally expressed in the neuroendocrine brain in a developmentally regulated and cell-specific fashion. Mol Cell Neurosci. 17(1): 107-26.
Li M et al. (1998). Testis-specific prohormone convertase PC4 processes the precursor of pituitary adenylate cyclase-activating polypeptide (PACAP). Peptides.19(2): 259-68.
Li M et al. (1999). Prohormone convertases 1 and 2 process ProPACAP and generate matured, bioactive PACAP38 and PACAP27 in transfected rat pituitary GH4C1 cells. Neuroendocrinology. 69(3): 217-26.
Li YC et al. (2004). Microsatellites within genes: structure, function, and evolution. Mol Biol Evol. 21(6): 991-1007.
Mathews DH et al. (1999). Expanded sequence dependence of thermodynamic parameters improves prediction of RNA secondary structure. J Mol Biol. 288: 911-940.
Miyata A et al. (1990). Isolation of a neuropeptide corresponding to the N-terminal 27 residues of the pituitary adenylate cyclase activating polypeptide with 38 residues (PACAP38). Biochem Biophys Res Commun. 170(2): 643-8.
Miyata A et al. (2000). Genomic organization and chromosomal localization of the mouse pituitary adenylate cyclase activating polypeptide (PACAP) gene. Ann N Y Acad Sci. 921: 344-8.
Miyata et al. (1989). Isolation of a novel 38 residue-hypothalamic polypeptide which stimulates adenylate cyclase in pituitary cells. Biochem Biophys Res Commun. 164(1): 567-74.
Montero M et al. (2000). Molecular evolution of the growth hormone-releasing hormone/pituitary adenylate cyclase-activating polypeptide gene family. Functional implication in the regulation of growth hormone secretion. J Mol Endocrinol. 25(2): 157-68.
Nijmeijer JS et al. (2010). Identifying loci for the overlap between attention-deficit/hyperactivity disorder and autism spectrum disorder using a genome-wide QTL linkage approach. J Am Acad Child Adolesc Psychiatry.

49(7): 675-85.
Nordheim A and Rich A (1983). The sequence (dC-dA)n X (dG-dT)n forms left-handed Z-DNA in negatively supercoiled plasmids. Proc Natl Acad Sci U S A. 80(7): 1821-5.
Norrholm SD et al. Behavioral effects of local microinfusion of pituitary adenylate cyclase activating polypeptide (PACAP) into the paraventricular nucleus of the hypothalamus (PVN). Regul Pept. 128(1): 33-41.
Ohkubo S et al. (1994). Expression of the PACAP gene in a human neuroblastoma cell line: cDNA cloning and analyses of the upstream regulatory region. Endocr J. 2:135--145.
Okazaki K et al. (1995). Characterization of murine PACAP mRNA. Peptides. 16(7): 1295-9.
Pe'rez-Jurado LA and Francke U (1993). Dinucleotide repeat polymorphism at the human pituitary adenylate cyclase activating polypeptide (PACAP) gene. Hum Mol Genet. 2(6): 827.
Pedersen AG and Nielsen H (1997). Neural network prediction of translation initiation sites in eukaryote perspectives for EST and genome analysis. Proc Int Conf Intell Syst Mol Biol. 5: 226-33.
Ressler KJ et al. (2011). Post-traumatic stress disorder is associated with PACAP and the PAC1 receptor. Nature. 470(7335): 492-7.
Rich A et al. (1984). The Chemistry and Biology of Left-Handed Z-DNA. Annu Rev Biochem. 53:791-846.
Rutherford S et al. (2004). Sibpair studies implicate chromosome 18 in essential hypertension. Am J Med Genet A. 126A(3): 241-7.
Sakai T et al. (2004). Update of mouse microsatellite database of Japan (MMDBJ). Exp Anim. 53(2): 151-4.
Somers J et al. (2013). A perspective on mammalian upstream open reading frame function. Int J Biochem Cell Biol. 45(8): 1690-700.
Stroth N and Eiden LE (2010). Stress hormone synthesis in mouse hypothalamus and adrenal gland triggered by restraint is dependent on pituitary adenylate cyclase-activating polypeptide signaling. Neuroscience. 165(4): 1025-30.
Tam JK et al. (2007). PACAP-related peptide (PRP)--molecular evolution and potential functions. Peptides. 28(9): 1920-9.
Tannous BA et al. (2005). Codon-optimized Gaussia luciferase cDNA for mammalian gene expression in culture and in vivo. Mol Ther. 11(3): 435-43.
Tominaga A et al. (2008). Implication of pituitary adenylate cyclase-activating polypeptide (PACAP) for neuroprotection of nicotinic acetylcholine receptor signaling in PC12 cells. J Mol Neurosci. 36(1-3): 73-8.
Vaudry D et al. (2000). Pituitary adenylate cyclase-activating polypeptide and its receptors: from structure to functions. Pharmacol Rev. 52(2): 269-324.
Vaudry D et al. (2009). Pituitary adenylate cyclase-activating polypeptide and its receptors: 20 years after the discovery. Pharmacol Rev. 61(3): 283-357.
Wade CM et al. (2002). The mosaic structure of variation in the laboratory mouse genome. Nature. 420(6915): 574-8.
Weintraub H (1983). A dominant role for DNA secondary structure in forming hypersensitive structures in chromatin. Cell. 32(4): 1191-203.
Wong E et al. (2002). Mbd4 inactivation increases Cright-arrowT transition mutations and promotes gastrointestinal tumor formation. Proc Natl Acad Sci U S A. 99(23): 14937-42.
Yamamoto K et al. (1998). Cloning and characterization of the mouse pituitary adenylate cyclase-activating polypeptide (PACAP) gene. Gene. 211(1): 63-9.
Zuker M (2003). Mfold web server for nucleic acid folding and hybridization prediction. Nucleic Acids Res. 31: 3406-3415.
de Felipe P and Ryan MD (2004). Targeting of proteins derived from self-processing polyproteins containing multiple signal sequences. Traffic. 5(8): 616-26.
van Oers JS et al. (2013). The MutSβ complex is a modulator of p53-driven tumorigenesis through its functions in both DNA double-strand break repair and mismatch repair. Oncogene. doi: 10.1038/onc.2013.365.

4. Acknowledgements

To perform this study and write up this thesis, I had numerous helps and supports from many people. This work could not be done without those helps and supports.

I would like to thank my supervisor Dr. Tsuyoshi Koide for his great advice and his mind of wide scope for my study. He let me study freely what I wanted to do, but he gave critical advice

when needed. I am grateful to Dr. Aki Takahashi for her unstinting support and advice. I thank Dr. Tatsuhiko Goto for his nice advices.

5. Figures and tables

Table 1. Primer sets used for genotyping.

		Location (bp)			Forward primer		Reverse primer					
Symbol	Location (cM)	Start		End	Sequence	Length (bp)	Sequence	Length (bp)	Product size (bp)	Entrez Gene ID	UniSTS ID	MGI ID
D17Mit164	2.11	3,924,615	39.24615	3,924,747	AGGCCCTAACATGTAGCAGG	20	TATTATTGAGACTGTGGTTGTTGTTG	26	133	n.a.	116474	705495
D17Mit81	15.80	30,904,398	309.04398	30,904,522	CAATCTATCTCATATGCATCTCTGTG	26	GTCTGGTGCACCTGTCCTC	19	125	n.a.	128106	705953
D17Mit34	18.31	34,744,053	347.44053	34,744,199	TGTTGGAGCTGAATACACGC	20	GGTCCTTGTTTATTCCCAGTACC	23	147	62228	128083	707736
D17Mit168	19.74	43,574,081	435.74081	43,574,223	ATGGTCCTGGAACATAGCCA	20	CTACATAGGCATGTGCATGACA	22	143	63024	127991	705493
D17Mit36	22.90	46,821,629	468.21629	46,821,740	ATCTCACCAGTCCTTGTTTTCTG	23	CCCCAGAATTTATGTGGTGG	20	112	n.a.	116656	703203
D17Mit9	26.61	51,168,551	511.68551	51,168,656	TCAGCCCTTAAAAATTACTCTTGG	24	CCCCACCAACTGTCCTCTAA	20	106	60982	116659	704217
D17Mit20	29.73	57,227,447	572.27447	57,227,623	AGAACAGGACACCGGACATC	20	TCATAAGTAGGCACACCAATGC	22	177	n.a.	128014	702760
D17Mit253	32.68	62,941,706	629.41706	62,941,936	GTGACTGAGGGAGTCATT	18	CAAGAGAATCACACATATTG	20	231	n.a.	128065	701161
D17NigT403	n.a.	64,677,390	646.77390	64,677,499	GGCTGAGTCTGAGAACTGCT	20	CGGAGAAATCCTGTCTCAAT	20	110	n.a.	n.a.	n.a.
D17Mit217	35.26	65,887,410	658.87410	65,887,530	TACCTTCTTGTTCTTAACTAACACACA	27	ATTTACAAGCACAGTTCAGTTGTG	24	121	n.a.	n.a.	702489
D17Mit3	39.08	68,143,589	681.43589	68,143,719	GATCTTTTCTTATTCTGGTT	20	GCAAAGTCATGTACTCTGAG	20	131	n.a.	116668	704226
D17NigT302	n.a.	72,216,918	722.16918	72,217,063	TGAGGCAGCAGACTTCATTA	20	ACACCTCCTTCTGGCCTATG	20	146	n.a.	n.a.	n.a.
D17Mit129	56.83	86,688,824	866.88824	86,688,972	TGTTGATTTCTGGTGTCCACA	21	GACAGGTTGAGCAACTCATCTG	22	149	62698	127961	705097
D17NigT103	n.a.	87,409,660	874.09660	87,409,780	ATTTGATCATTTCCCCACCT	20	AATGCCAAAATTACAGTTTTCA	22	121	n.a.	n.a.	n.a.
D17Mit221	59.77	90,087,705	900.87705	90,087,842	AACCAGATCATTAACAGTAATAAAGCA	27	TTGTGGCAAAAACAACCAAA	20	138	n.a.	128037	706544
D17NigT115	n.a.	91,095,892	910.95892	91,096,041	CTACTTAAAATGAAAGAAACATCACAG	27	GCAAAACAAAACATAAACCCAAA	23	150	n.a.	n.a.	n.a.
D17NigT116	n.a.	91,587,850	915.87850	91,588,000	TGAGAAAACAGAATGTAAGACTTTTCC	27	GGGTGGTGGTGAAATGTGTA	20	151	n.a.	n.a.	n.a.
D17NigT116.5	n.a.	91,909,183	919.09183	91,909,397	CAAAAGCACCCATACTGTCCTG	22	CCTTCATTCCTGCCTGATGTG	21	215	n.a.	n.a.	n.a.
D17Mit123	60.67	93,199,619	931.99619	93,199,751	CACAAGGAGGGAGCCTGTAG	20	CACCGTAAGAGTCTAATAATAAGGGG	26	133	62697	116680	705091
D17Nig119	n.a.	94,190,165	941.90165	94,190,289	GATTCTCTCCTCTCAGGTTGACAT	24	CTTCCCTTTCTTCCCTCTGC	20	125	n.a.	n.a.	n.a.

n.a., not-available.

Table 2. Primer sets used for quantitative real-time PCR and RT-PCR.

Target gene (region)	Reference Sequence ID	Forward primer Name (sequence)	Length (bp)	Reverse primer Name (sequence)	Length (bp)	Product size (bp)	Roche universal probe no.	Takara primer set ID	Reference article
β actin	NM_007393	Beta-actin F (TGACAGGATGCAGAAGGAGA)	20	Beta-actin R(CGCTCAGGAGGAGCAATG)	18	75	106		
Gapdh	NM_001289726	ACCACAGTCCATGCCATCAC	20	TCCACCACCCTGTTGCTGTA	20	452			
Nrxn1	NM_020252	Nrxn1 F (CCACCTCAATCATGGAGACC)	20	Nrxn1 R(GGGTCAATGTCCTCATCGTC)	29	148			
PACAP (3-4)	NM_009625	MA027807 F	24	MA027807 R	21	125		MA027807	
PACAP (1A-5)		PACAP_i (GCCTGAGACCTCAGAGCAGA)	20	PACAP_v (CTACAAGTATGCTATTCGGCGTCC)	24				
PACAP (1A-2)		PACAP_ii (AGAGCAGAGAAGAATGACCATGTG)	24	PACAP_iv (GATCCCAGGGAAGCTGAGTC)	20	118			
PACAP (1B-2)		PACAP_iii (GCTGTCCTACTTAGTCAACCCTTTC)	25	PACAP_iv (GATCCCAGGGAAGCTGAGTC)	20	140			
Adcyap1r1	NM_001025372	Adcyap1r1 F (CCCTGGCATGTGGGACAA)	18	Adcyap1r1 R (GGCAGCTTACAAGGACCA)	18	71			Apostolakis et al., 2005
Mettl4	NM_176917	MA068162-F	23	MA068162-R	20	84		MA068162	

Table 3. Behavioral profiles in congenic strains.

Test	B6	T103	T103–T116	T116	T119
Novel cage					
Activity (events/60min)	2,113 ± 110	1,855 ± 170	1,922 ± 172	1,672 ± 140*	n.a.
Home cage					
Activity (events/ 1 day)	12,718 ± 688	14,419 ± 833	12,164 ± 1165	10,800 ± 904*	n.a.
Open field					
Activity (events / 10min)	5,366 ± 275	5,169 ± 230	5,082 ± 388	4,161 ± 161*	4,886 ± 313
Center time (s)	10.0 ± 0.8	11.7 ± 1.3	8.9 ± 0.7	12.1 ± 1.8	9.5 ± 1.8
Light dark box					
Activity in light box (events /	1,500 ± 106	1,357 ± 95	1,508 ± 163	1,472 ± 127	n.a.
Activity in dark box (events /	2,435 ± 86	2,399 ± 136	2,269 ± 120	2,105 ± 189*	n.a.
Time spent in light box (%)	33.9 ± 2.0	33.6 ± 3.8	38.2 ± 3.5	42.6 ± 5.0	n.a.
Latency of dark box entry (s)	79 ± 10	83 ± 26	104 ± 23	118 ± 38	n.a.
Transition count	29 ± 2	27 ± 3	29 ± 4	26 ± 4	n.a.
Elevated plus maze					
Activity (events / 10min)	1,542 ± 80	1,171 ± 72*	1,405 ± 118	1,164 ± 69*	n.a.
Open arms time (%)	21.7 ± 2.4	20.9 ± 4.1	18.0 ± 3.0	15.4 ± 4.5	n.a.
Light enhanced startle response					
Dark condition	167.4 ± 17.5	178.5 ± 19.5	199.6 ± 22.0	197.5 ± 12.4	—
Light condition	216.1 ± 18.5	216.8 ± 24.9	256.4 ± 32.1	224.4 ± 18.0	—
Difference	48.6 ± 11.8	38.3 ± 15.1	56.9 ± 22.4	26.9 ± 13.6	n.a.

n.a., not-available.

Table 4. Candidate genes in T116-T119 locus.

Location (bp)						
Start	Stop	Length (bp)	Symbol	Gene type	MGI	Description
91,666,767	91,673,748	6,982	Gm15403	pseudo	3641944	protein-L-isoaspartate (D-aspartate) O-methyltransferase domain containing 1 pseudogene
91,781,292	91,782,486	1,195	Gm19856	pseudo	5012041	UPF0711 protein C18orf21 homolog
92,185,388	92,185,957	570	Gm19145	pseudo	5011330	ubiquitin-conjugating enzyme E2E 1, UBC4/5 homolog pseudogene
92,372,015	92,373,117	1,103	Gm6751	pseudo	3647438	actin, gamma, cytoplasmic 1 pseudogene
92,717,885	92,719,072	1,188	Gm21018	pseudo	5434373	pyruvate kinase, muscle pseudogene
93,199,422	93,205,491	6,070	Adcyap1	protein coding	105094	adenylate cyclase activating polypeptide 1
93,316,720	93,317,261	542	Gm9665	pseudo	3780073	ribosomal protein L3 pseudogene
93,331,383	93,332,952	1,570	Gm6764	pseudo	3644641	PWP1 homolog pseudogene

Table 5. Genetic differences in the PACAP gene between B6 and MSM stains.

dbSNP rs number	Location (bp)	Annotation	Variant Type	Alleles (B6/MSM)
rs244186985	93,194,055	Upstream	INDEL	T/−
rs46953537	93,194,094	Upstream	SNP	G/T
n.a.	93,194,341	Upstream	INDEL	(T)19/−
rs45677001	93,194,393	Upstream	SNP	G/T
rs6397044	93,194,832	Upstream	SNP	A/G
rs51430910	93,195,609	Upstream	SNP	T/C
rs226243879	93,195,675	Upstream	SNP	A/G
rs46177478	93,195,987	Upstream	SNP	G/C
rs48660253	93,196,126	Upstream	SNP	A/T
rs45740909	93,196,567	Upstream	SNP	G/A
rs50305996	93,196,665	Upstream	SNP	C/T
n.a.	93,196,802	Upstream	Microsatellite	n.a.
rs46417390	93,197,441	Upstream	SNP	A/G
n.a.	93,197,620	Upstream	Microsatellite	n.a.
rs3664454	93,198,693	Upstream	SNP	T/G
rs50376855	93,198,879	Upstream	SNP	G/A
rs234724157	93,199,204	Intron 1	INDEL	−/CCGACTC
n.a.	93,199,275	Intron 1	INDEL	CACT/−
rs3023460	93,199,618	Exon 1B (5U)	SNP	A/C
n.a.	93,199,647	Intron 2	Microsatellite	−/TG
rs107924446	93,199,667	Intron 2	Microsatellite	T/C
n.a.	93,199,669	Intron 2	Microsatellite	−/(TG)13
rs48538506	93,199,848	Intron 2	SNP	T/C
rs264353789	93,199,912	Intron 2	SNP	G/C
rs229418381	93,199,946	Intron 2	SNP	C/G
rs51087440	93,200,149	Intron 3	SNP	T/C
rs51441467	93,200,178	Intron 3	SNP	A/G
rs45669295	93,200,211	Intron 3	SNP	A/G
rs246539499	93,200,771	Intron 3	SNP	T/A
rs247406100	93,201,029	Intron 3	SNP	G/A
n.a.	93,201,191	Intron 3	INDEL	G/−
n.a.	93,201,566	Intron 3	SNP	T/C
rs49752584	93,202,924	Intron 5	SNP	C/T
rs47803731	93,202,990	Intron 5	SNP	G/A
rs51037596	93,203,076	Intron 5	SNP	A/T
rs48349145	93,203,316	Intron 5	SNP	C/A
rs46194300	93,203,481	Intron 5	SNP	A/T
rs49835159	93,203,628	Intron 5	SNP	A/G
rs214552052	93,203,735	Intron 5	SNP	G/T
rs33584965	93,204,387	Exon 5 (U3)	SNP	T/A
rs222996636	93,204,991	Exon 5 (U3)	SNP	A/G
rs261447293	93,205,265	Exon 5 (U3)	SNP	G/A
n.a.	93,205,816	Exon 5 (U3)	INDEL	A/−
rs50650668	93,206,118	Exon 5 (U3)	SNP	T/A
rs258107575	93,206,564	Downstream	INDEX	A/−
rs46291770	93,206,861	Downstream	SNP	G/C
rs49198218	93,207,086	Downstream	SNP	A/G
rs235714627	93,207,188	Downstream	SNP	A/G
rs255396806	93,207,200	Downstream	SNP	C/T
rs221093830	93,207,210	Downstream	SNP	T/A
rs241372658	93,207,259	Downstream	SNP	C/T
rs265090444	93,207,333	Downstream	SNP	G/A
rs244469288	93,207,415	Downstream	SNP	G/T
rs228721901	93,207,461	Downstream	SNP	T/C
rs247226396	93,207,478	Downstream	SNP	C/A
rs227358086	93,207,578	Downstream	SNP	T/C
rs250402814	93,207,633	Downstream	SNP	T/C
rs214737759	93,207,634	Downstream	SNP	G/A

n.a., not-available. U5, a UTR variant of the 5' UTR. U3, a UTR variant of the 3' UTR.

Table 6. Polymorphisms in PACAP gene between laboratory and wild-derived strains.

	Origin		Genotype rs3023460 (A/C)	93199647 (TG)n	
Strain	Subspecies group	Place		Sequence	Length (bp)
Laboratory					
C57BL/6J	*M. m. domesticus*		A	$(TG)_{26}$	52
C58/J	*M. m. domesticus*		A	$(TG)_{26}$	52
HRS/J	*M. m. domesticus*		n.a.	$(TG)_{26}$	52
TF/GnLe	*M. m. domesticus*		n.a.	$(TG)_{26}$	52
BALB/cUcsd	*M. m. domesticus*		A	$(TG)_{27}$	54
C57BL/10SnJ	*M. m. domesticus*		A	$(TG)_{28}$	56
A/J	*M. m. domesticus*		A	$(TG)_{29}$	58
129/SvJ	*M. m. domesticus*		A	$(TG)_{29}$	58
CBA/J	*M. m. domesticus*		A	$(TG)_{30}$	60
CE/J	*M. m. domesticus*		C	$(TG)_{10}CG(TG)_{21}$	64
RBF/DnJ	*M. m. domesticus*		C	$(TG)_{10}CG(TG)_{22}$	66
SWR/J	*M. m. domesticus*		C	$(TG)_{10}CG(TG)_{23}$	68
MA/MyJ	*M. m. domesticus*		C	$(TG)_{10}CG(TG)_{25}$	72
PL/J	*M. m. domesticus*		C	$(TG)_{10}CG(TG)_{25}$	72
NZB/San	*M. m. domesticus*		C	$(TG)_{9}CG(TG)_{26}$	72
PT/7af	*M. m. domesticus*		C	$(TG)_{10}CG(TG)_{25}$	72
I/LnJ	*M. m. domesticus*		C	$(TG)_{10}CG(TG)_{25}$	72
SM/J	*M. m. domesticus*		C	$(TG)_{10}CG(TG)_{25}$	72
DBA/2J	*M. m. domesticus*		C	$(TG)_{10}CG(TG)_{25}$	72
AKR/J	*M. m. domesticus*		C	$(TG)_{10}CG(TG)_{25}$	72
C57L/J	*M. m. domesticus*		C	$(TG)_{10}CG(TG)_{25}$	72
P/J	*M. m. domesticus*		C	$(TG)_{11}CG(TG)_{24}$	72
RIIIS/J	*M. m. domesticus*		C	$(TG)_{10}CG(TG)_{25}$	72
C3H/HeJ	*M. m. domesticus*		C	$(TG)_{10}CG(TG)_{25}$	72
DBA/1J	*M. m. domesticus*		C	$(TG)_{10}CG(TG)_{27}$	76
Wild-derived					
AVZ/Ms	*M. m. bactrianus*	Iran	C	$(TG)_{27}$	54
CAST/Ei	*M. m. castaneus*	Thailand	C	$(TG)_{10}CG(TG)_{30}$	82
HMI/Ms	*M. m. castaneus*	Heimei, Taiwan	C	$(TG)_{7}(CG)_{3}(TG)_{6}TA(TG)_{37}$	108
MAL/Ms	*M. m. castaneus*	Malaysia	C	$(TG)_{7}(CG)_{3}(TG)_{6}TA(TG)_{40}$	114
PGN2/Ms	*M. m. domesticus*	Pegion, Canada	n.a.	$(TG)_{10}CG(TG)_{27}$	76
SK/Cam	*M. m. domesticus*	Skokholm Island, England	n.a.	$(TG)_{10}CG(TG)_{29}$	80
BFM/2Ms	*M. m. domesticus*	Montpellier, France	n.a.	$(TG)_{10}CG(TG)_{30}$	82
MSM/Ms	*M. m. molossinus*	Mishima, Japan	C	$(TG)_{11}CG(TG)_{28}$	80
NJL/Ms	*M. m. musculus*	Northern Jutland, Denmark	C	$(TG)_{11}CG(TG)_{3}CG(TG)_{20}$	72
BLG2/Ms	*M. m. musculus*	Toshevo, Bulgaria	C	$(TG)_{13}CG(TG)_{26}$	80
KJR/Ms	*M. m. subspecies*	Kojuri, Korea	C	$(TG)_{11}CG(TG)_{23}$	70
SWN/Ms	*M. m. subspecies*	Suwon, Korea	C	$(TG)_{11}CG(TG)_{24}$	72
CHD/Ms	*M. m. subspecies*	Chendu, China	C	$(TG)_{12}CG(TG)_{28}$	82
Fancy mice					
JF1/Ms	*M. m. molossinus*	Japan	C	$(TG)_{11}CG(TG)_{28}$	80
Outgroup					
ZBN/Ms	*M. m. spicilegus*	Bulgaria	n.a.	$(TG)_{27}(CGTG)_{2}TGCG(TGTA)_{3}(TG)_{7}$	92
STF/Pas	*M. m. spretus*	Fondouk el Djedid, Tunisia	n.a.	n.a.	72*
SEG/Pas	*M. m. spretus*	Grenada, Spain	n.a.	n.a.	92*
SPRET/Ei	*M. m. spretus*	Cadiz, Spain	C	n.a.	97*

n.a., not-available. *, data were obtained from Mouse Microsatellite Data Base of Japan (MMDBJ).

Table 7. Probabilities of translation start site in the PACAP splice variants.

	uORF1 (%)	uORF2 (%)	Main ORF (%)
PACAP splice variant 1	0.468	0.381	0.383
PACAP splice variant 2	0.468	0.259	0.383
PACAP splice variant 3	0.468	n.a.	0.527

n.a., not-available.

Table 8. List of loci separated in the nucleotide length of microsatellite between laboratory and wild-derived strains.

Locus name	Chr.	Intragenic	Intergenic	Description	ttest
D5Mit4	5		Acox3	acyl-Coenzyme A oxidase 3, pristanoyl	1.6E-05
D6Mit266	6	Kcnd2		potassium voltage-gated channel, Shal-related family, member 2	2.5E-05
D11Mit212	11		Akap1	A kinase (PRKA) anchor protein 1 (Akap1)	3.2E-04
D6Mit22	6	EG545861		predicted gene, EG545861	6.6E-04
D8Mit256	8		LOC624710	similar to Katanin p60 ATPase-containing subunit A1 (Katanin p60 sub	9.2E-04
D15Mit6	15		Azin1 Siah1-ps2	antizyme inhibitor 1 seven in absentia 1, pseudogene 2	1.2E-03
D17Mit81	17	Glp1r		glucagon-like peptide 1 receptor	2.4E-03
D10Mit150	10		LOC667855	similar to ribosomal protein L21	2.8E-03
D11Mit149	11		LOC100042722	hypothetical protein LOC100042722	3.1E-03
D17Mit123	17	Adcyap1		adenylate cyclase activating polypeptide 1	3.5E-03
D18Mit64	18	Arhgap12		Rho GTPase activating protein 12	4.3E-03
D17Mit20	17	C3		complement component 3	4.9E-03
D17Mit89	17		LOC638867	similar to suppressor of initiator codon mutations, related sequence 1	6.1E-03
D3Mit117	3		EG667759	predicted gene, EG667759	7.9E-03
D2Mit15	2		Creb3l1	cAMP responsive element binding protein 3-like 1	8.2E-03
D18Mit51	18	Hmgxb3		HMG box domain containing 3	9.0E-03
D15Mit60	15		Trhr	Thyrotropin releasing hormone receptor	9.5E-03
D18Mit142	18	Smad7		MAD homolog 7 (Drosophila)	1.4E-02
D2Mit82	2	Gpsm1		G-protein signalling modulator 1 (AGS3-like, C. elegans)	1.4E-02
D2Mit37	2	Hoxd10		homeo box D10	1.5E-02
D10Mit28	10		LOC666636	similar to ribosomal protein L27	1.6E-02
D6Mit4	6		LOC100043390	similar to antigen LEC-A	1.7E-02
D15Mit241	15		LOC100042309	similar to H3 histone, family 3A	1.9E-02
D1Mit444	1		LOC666983	hypothetical protein LOC666983	2.0E-02
D14Nki1	14	Rb1		retinoblastoma 1	2.0E-02
D11Mit141	11	Fstl4		follistatin-like 4	2.0E-02
D11Mit79	11		Glns-ps1	glutamine synthetase pseudogene 1	2.9E-02
D9Mit99	9		Tmprss5	transmembrane protease, serine 5 (spinesin)	3.6E-02

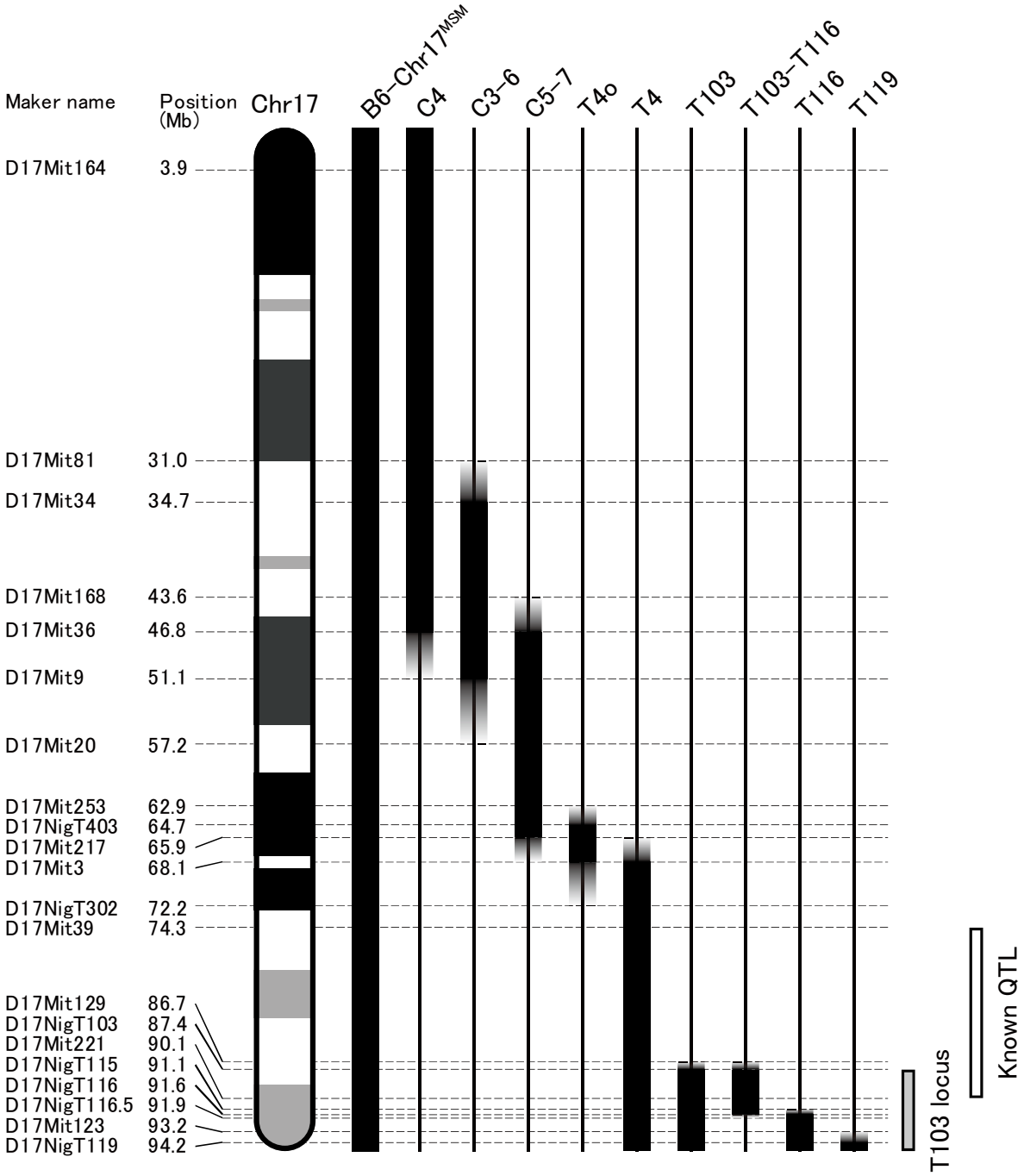

Figure 1. Schematic genome structures of chromosome 17 in the B6-Chr17^{MSM}, the sub-consomic, and the congenic strains. The genome structures of B6-Chr17^{MSM}, C4, C3-6, C5-7, T4o, T4, T103, T103-T116, T116, and T119 strains are shown. Black bars indicate loci derived from MSM. Gradational bars represent the undecided regions of genotypes. Texts and numbers on the left and the corresponding horizontal lines mean physical position of each genetic marker. Gray-colored box shows a QTL region of the T103 locus. White-colored box shows an

already-known QTL region identified in previous study (Singer JB et al. 2005). This map is according to reference assembly (GRCm38.p1).

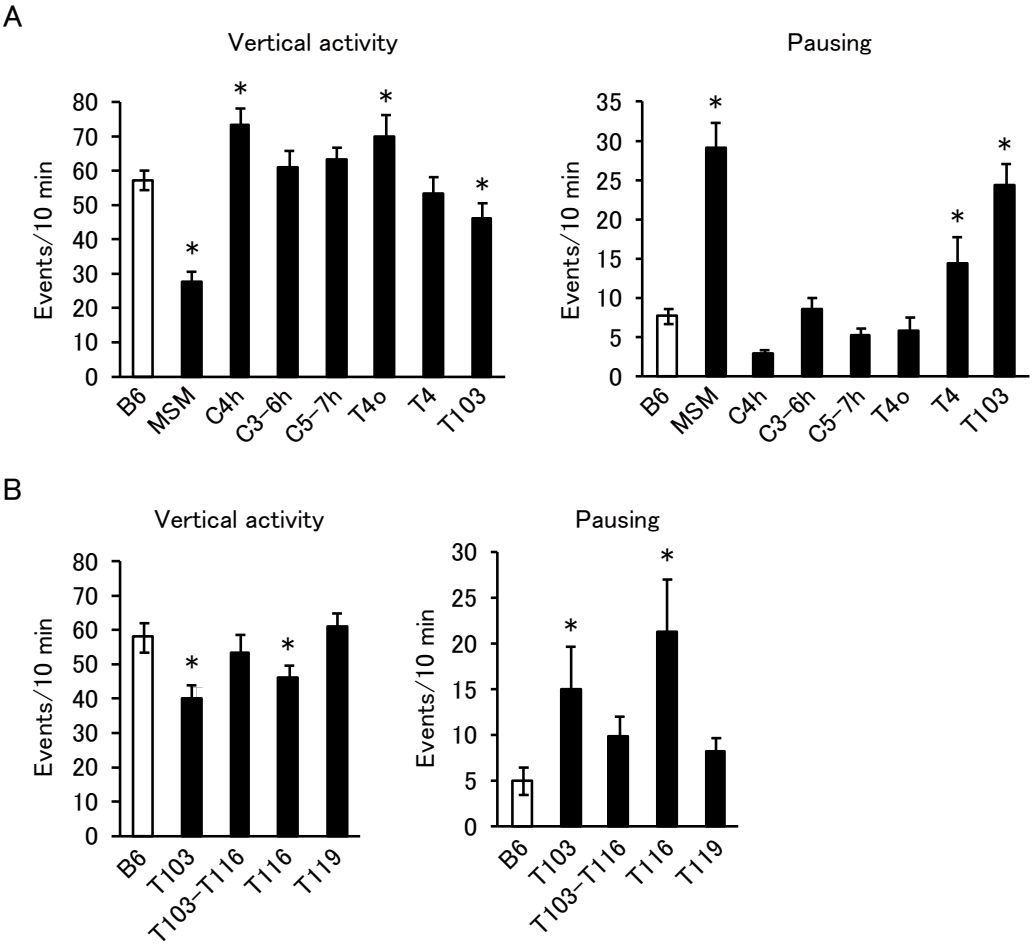

Figure 2. Genetic screening for behavioral responses to stress. Vertical activities and pausing behaviors were counted in open-field tests. (A) Systematic set of strains including B6, MSM, and the sub-consomic, and the congenic mice were used. n = 56 animals/group for B6 mice; n = 16-26 animals/group for others. (B) Particular strains including B6 and congenic mice were used for narrow down the QTL locus. n = 30 animals/group for B6 mice; n = 15-20 animals/group for others. Events/10 min means the total number of the behavior during the 10 min open-field test. Data are presented as mean ± SEM. **P* < 0.05 vs. B6 mice.

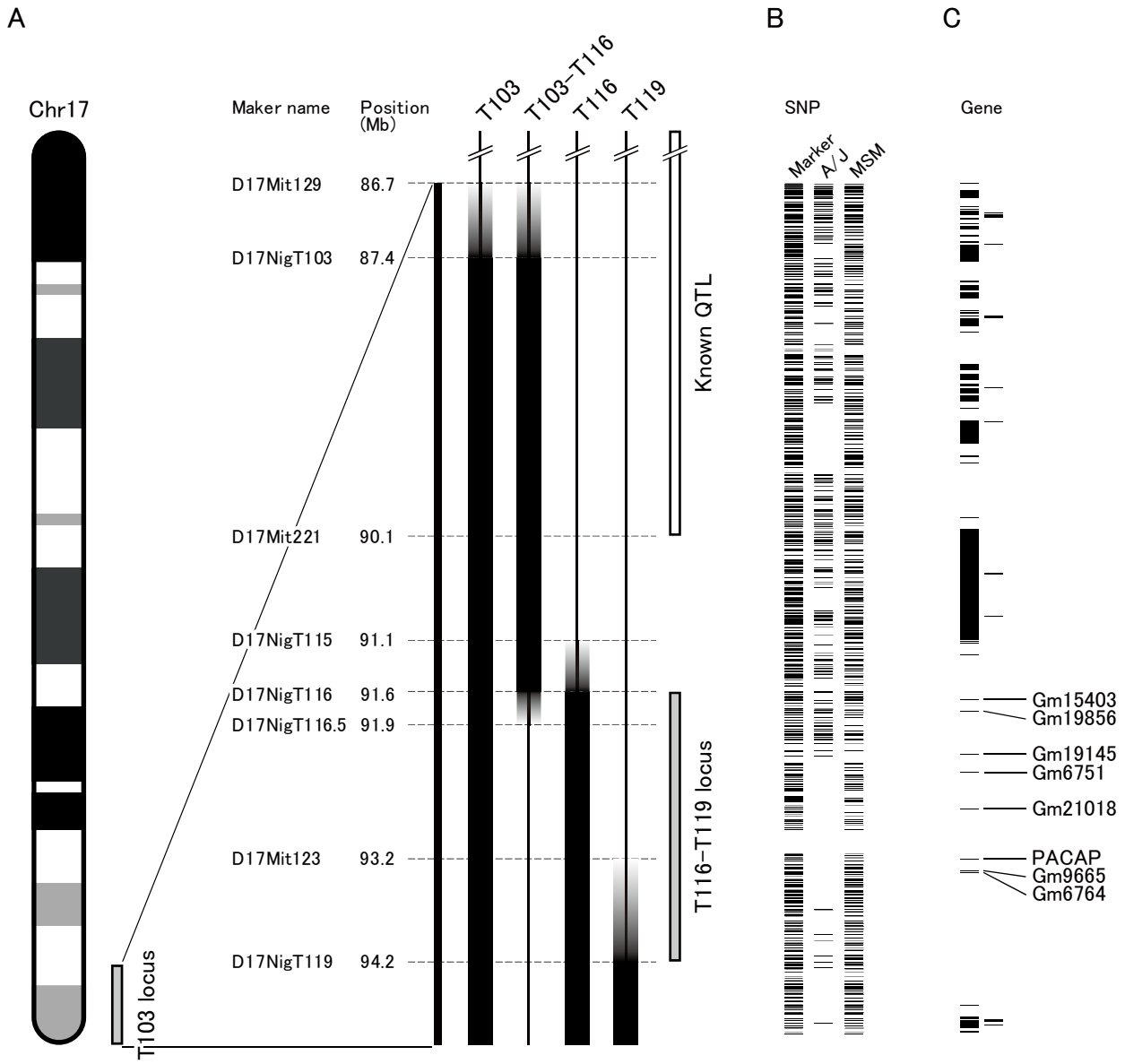

Figure 3. Schematic genome structures of chromosome 17 focused on the T103 locus. (A) The genome structures of T103, T103-T116, T116, and T119 strains are shown. See caption of Figure 1 for more details. (B) SNP markers and SNPs in A/J and MSM mice against the B6 reference are shown as horizontal bars corresponding to the genomic positions on the panel A. Genotype data were obtained from The Center for Genome Dynamics (http://cgd.jax.org/datasets/popgen/diversityarray/yang2011.shtml) and the physical positions of each SNP were obtained from dbSNP (http://www.ncbi.nlm.nih.gov/projects/SNP/). (C) The genes are indicated as black-colored boxes with symbols corresponding to the genomic positions on the panel A. Information of each gene was obtained from NCBI Annotation Release 104.

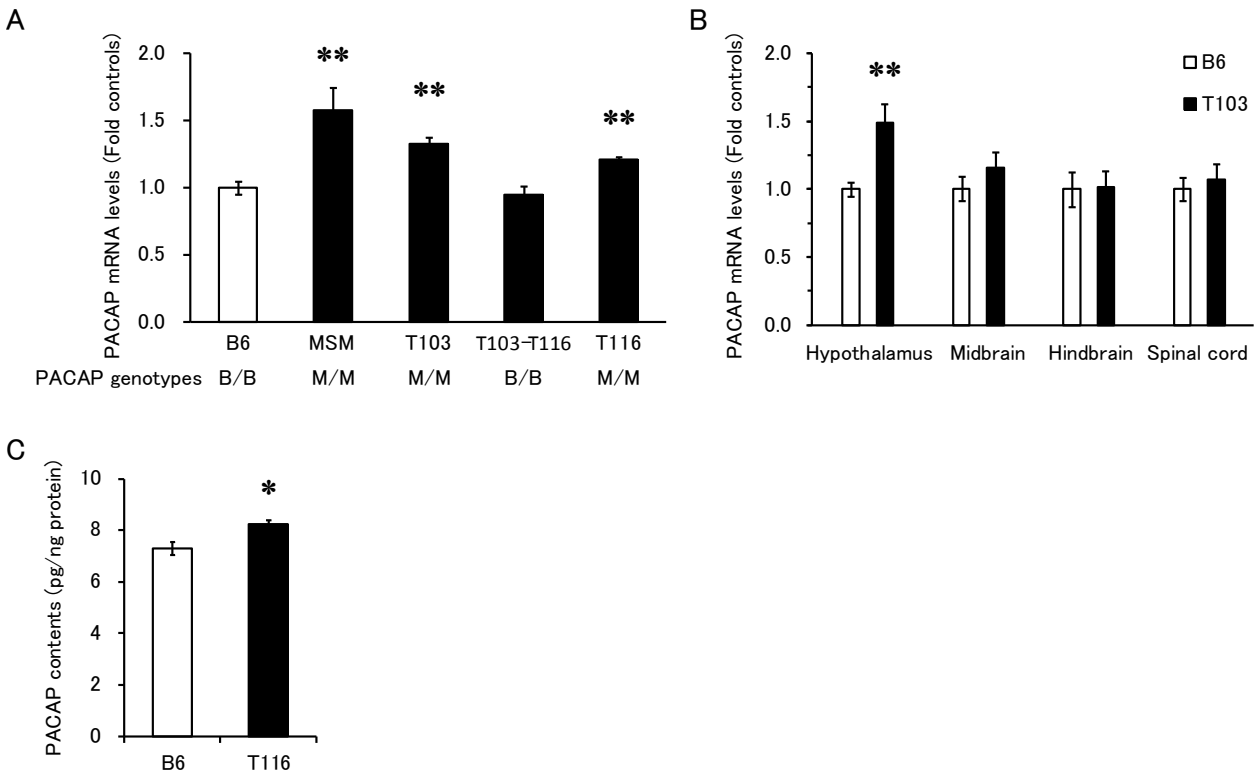

Figure 4. Strain differences of PACAP expression levels. PACAP mRNA levels were measured by quantitative real-time PCR using the total RNAs isolated from the whole brain of B6, MSM, T103, T103-T116, and T116 mice (A) and the hypothalamus, midbrain, hindbrain, and spinal cord of B6 and T103 mice (B). Data are normalized across samples against β-actin mRNA levels. B, B6 genotype; M, MSM genotype. (C) Radioimmunoassay for PACAP contents in hypothalamus in B6 and T116 mice. Data were normalized to the contents of soluble protein in the lysate. n = 5 animals/group. Data are presented as mean ± SEM. *$P < 0.005$, **$P < 0.001$ vs. B6 mice.

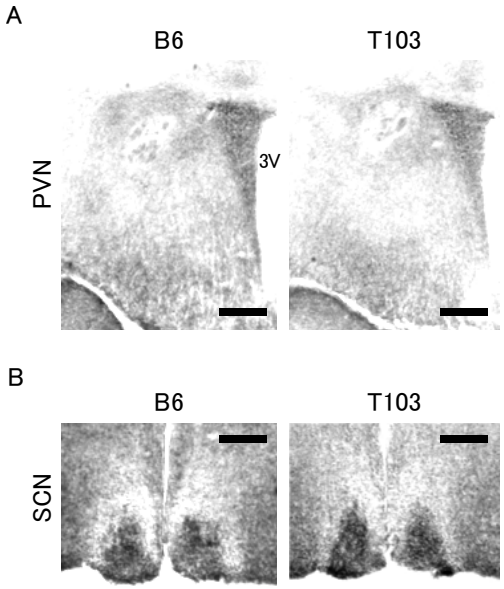

Figure 5. Normal distribution of PACAP-38 in hypothalamus in T103 mice. Representative sections immunolabeled by anti-PACAP-38 antibody in PVN (A) and the SCN (B) in hypothalamus of B6 and T103 mice. PVN, paraventricular nucleus; 3V, third cerebral ventricle; SCN, suprachiasmatic nucleus. Scale bars are 100 μm.

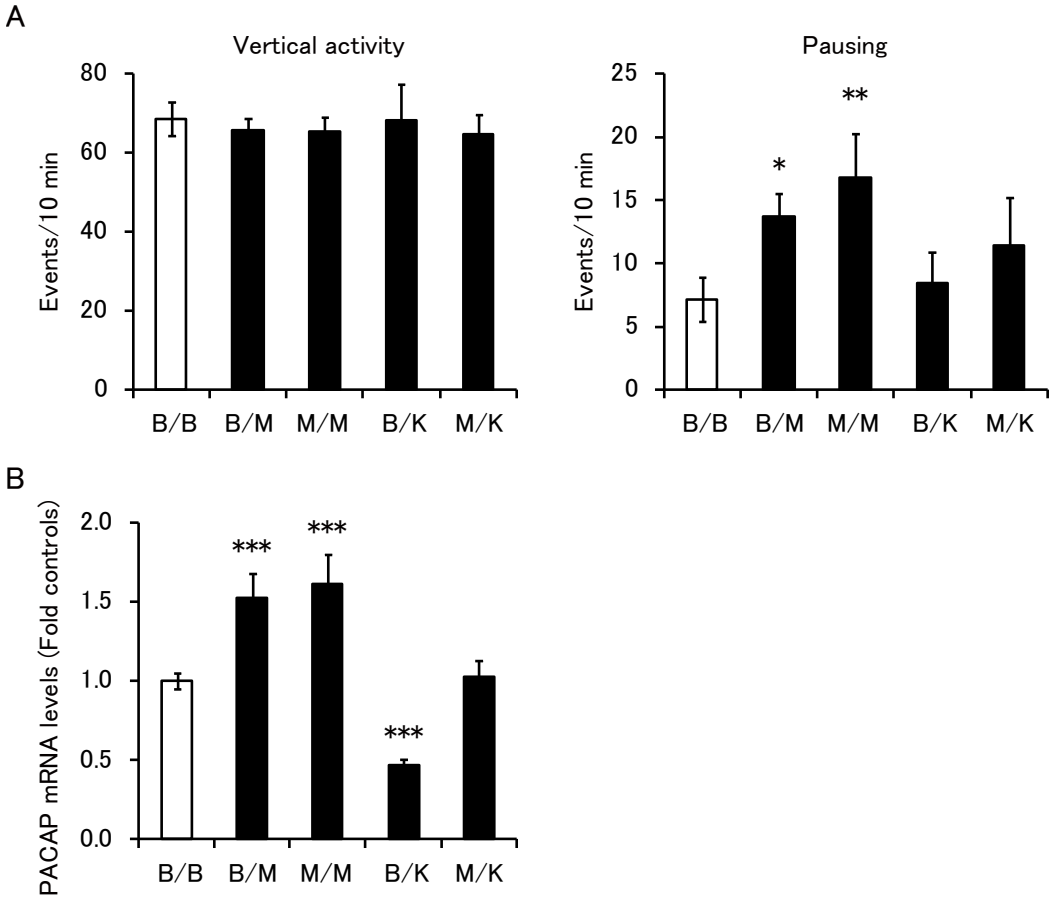

Figure 6. Pausing behaviors depended on the PACAP genotypes with the PACAP mRNA levels in (B6 x T116 F2) F2 and (B6 x T116) F1 x (B6 x PACAP-KO) F1 mice. (A) Vertical activities and pausing behaviors were counted in the open-field tests. n = 12-34 animals/group. Events/10 min means the total number of the behavior during the 10 min open-field tests. (B) PACAP mRNA levels were measured by quantitative real-time PCR using the total RNAs isolated from hypothalamus of each mouse. Data are normalized across samples against β-actin mRNA levels. n = 5-6 animals/group. B, B6 genotype; M, MSM genotype; K, PACAP-KO genotype. Data are presented as mean ± SEM. **P* < 0.05, ***P* < 0.01, ****P* < 0.001 vs. B/B genotypes.

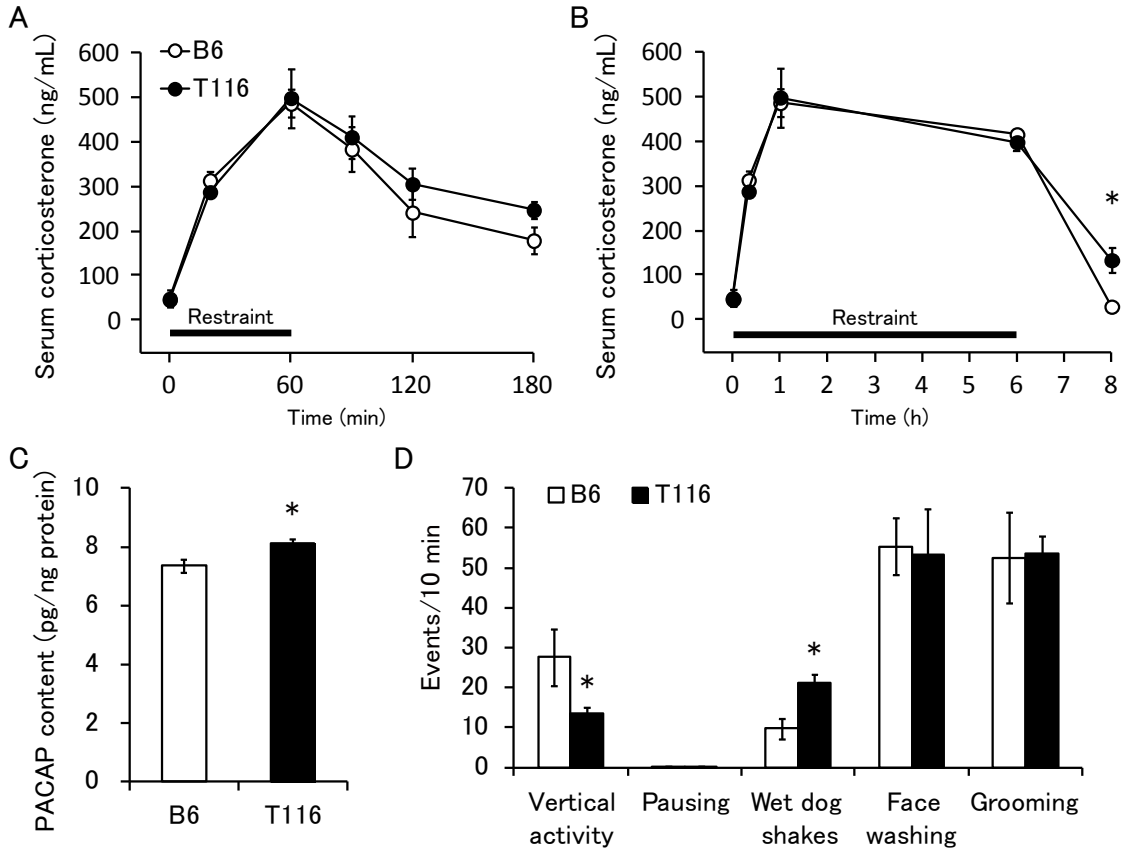

Figure 7. Normal corticosterone response to restrained stress and prolonged elevation of the corticosterone levels in T116 mice. Serum corticosterone levels were measured during and following the 1 hour stress (A) and 6 hour stress (B) in B6 (open circles) and T116 (closed circles) mice. Horizontal bar represents restraint period. n = 6-12 animals/group. (C) Radioimmunoassay for PACAP contents in hypothalamus in B6 and T116 mice following the stress. Data were normalized to the contents of soluble protein in the lysate. n = 5 animals/group. (D) Behavioral phenotypes were counted in open-field tests following the 6h restrained stress in B6 (open bars) and T116 (closed bars) mice. n = 12 animals/group. Events/10 min means the total number of the behavior during the 10 min open-field tests. Data are presented as mean ± SEM. **P* < 0.05 vs. B6 mice.

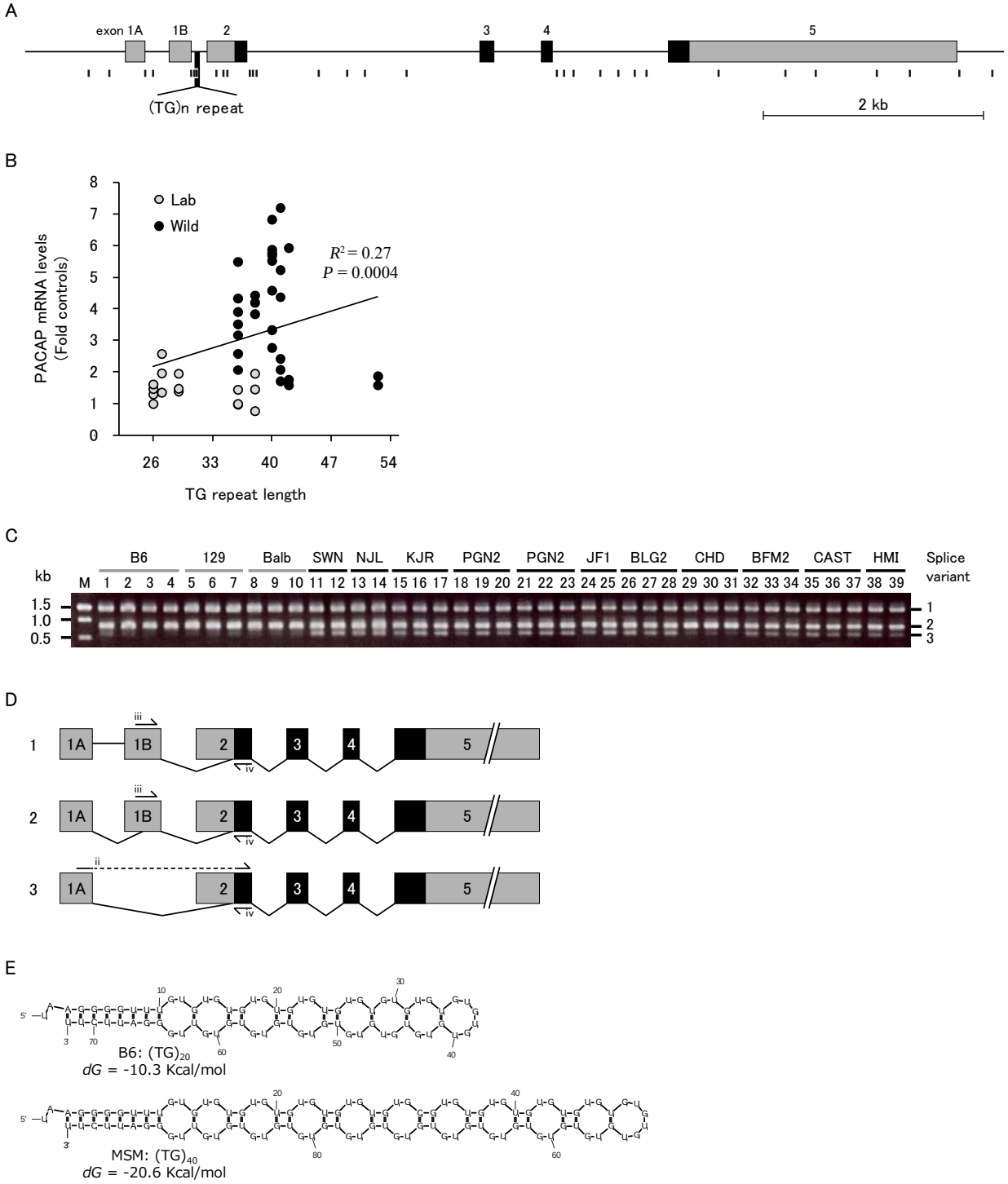

Figure 8. PACAP expression levels among several mouse strains. (A) Schematic structure of PACAP gene. Exons and introns are indicated as boxes and bars, respectively. Names of each exon are shown on the top. Non-coding and coding regions of the exons are showed by grey-colored and black-colored boxes, respectively. Polymorphisms including SNPs, insertions, and deletions between B6 and MSM strains shown by bars at the bottom corresponding to the

positions. The figure is a modification of the figure presented in GenBank track in USCS Genome Browser. (B) Correlation between PACAP mRNA levels and TG repeat lengths in a number of mouse strains. Results for the TG repeat lengths are plotted on the x-axis and for the PACAP mRNA levels on y-axis. Laboratory (grey circles) and wild-derived (closed circles) mice were used for this analysis. The TG repeat lengths were measured by direct sequencing of genome DNA of each strain. The PACAP mRNA levels were measured by quantitative real-time PCR using the total RNAs isolated from hypothalamus in each mouse. Data are normalized across samples against β-actin mRNA levels. (C) PACAP transcripts were amplified by reverse-transcript PCR using total RNAs isolated from hypothalamus in a number of mouse strains. Laboratory (grey bars) and wild-derived (black bars) mice were used for this analysis. The PCR products of each mouse (lane 1 to 39) were electrophoresed. DNA sizes are indicated on the left. Names of PACAP splice variants corresponding to the bands were indicated on the right. (D) Schematic structures of the PACAP transcripts. Primer sets used for reverse-transcript PCR and quantitative real-time PCR are indicated as arrows in corresponding to the positions. Names of the PACAP splice variants are indicated on the left. (E) Schematic illustration of RNA structures of the flanking sequence of the TG repeats in the PACAP intron 2 between B6 and MSM strains. Thermodynamic stabilities of the RNAs were predicted by mfold 3.4.

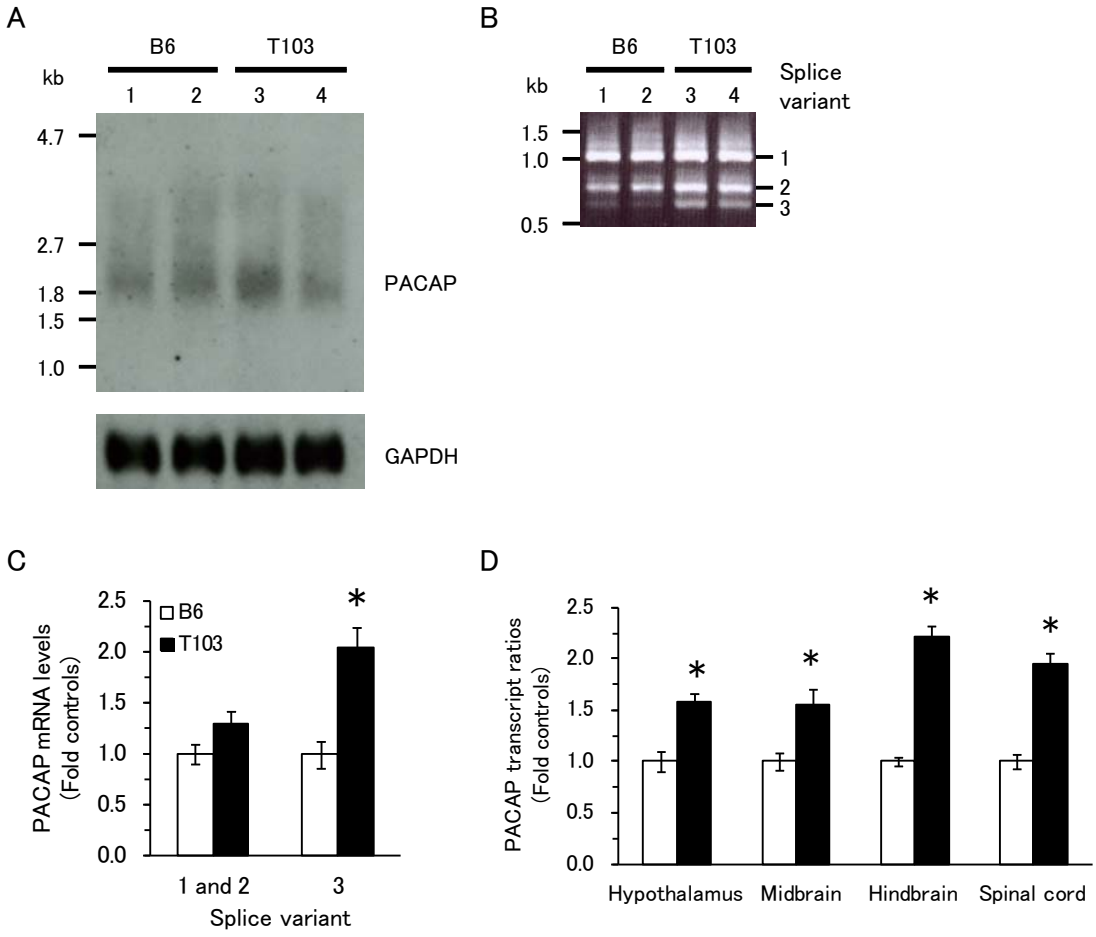

Figure 9. Altered expression profile of PACAP gene in T103 mice. (A) PACAP transcripts were detected by Northern blotting in B6 and T103 mice. Poly(A)+ mRNA in hypothalamus of B6 (lane 1 and 2) and T103 (lane 3 and 4) were blotted. GAPDH was used as control. (B) The PACAP transcripts were amplified by reverse-transcript PCR using total RNAs isolated from hypothalamus of B6 and T103 mice. The PCR products of B6 (lane 1 and 2) and T103 (lane 3 and 4) were electrophoresed. DNA sizes are indicated on the left. Names of PACAP splice variants corresponding to the bands were indicated on the right. (C) The PACAP transcript levels of each splice variant were measured by quantitative real-time PCR using the total RNAs isolated from hypothalamus of B6 and T103 mice. n = 5 animals/group. Data are normalized across samples against β-actin mRNA. (D) Ratios of mRNA levels of the PACAP splice variant 3 to PACAP splice variant 1 and 2 were measured by quantitative real-time PCR using the total RNAs isolated from hypothalamus, midbrain, hindbrain, and spinal cord of in B6 and T103 mice.

n = 5 animals/group. Data are normalized across samples against β-actin mRNA and PACAP splice variant 1 and 2. (C-D) Data are displayed as mean ± SEM. *, $P < 0.005$ vs. B6 mice.

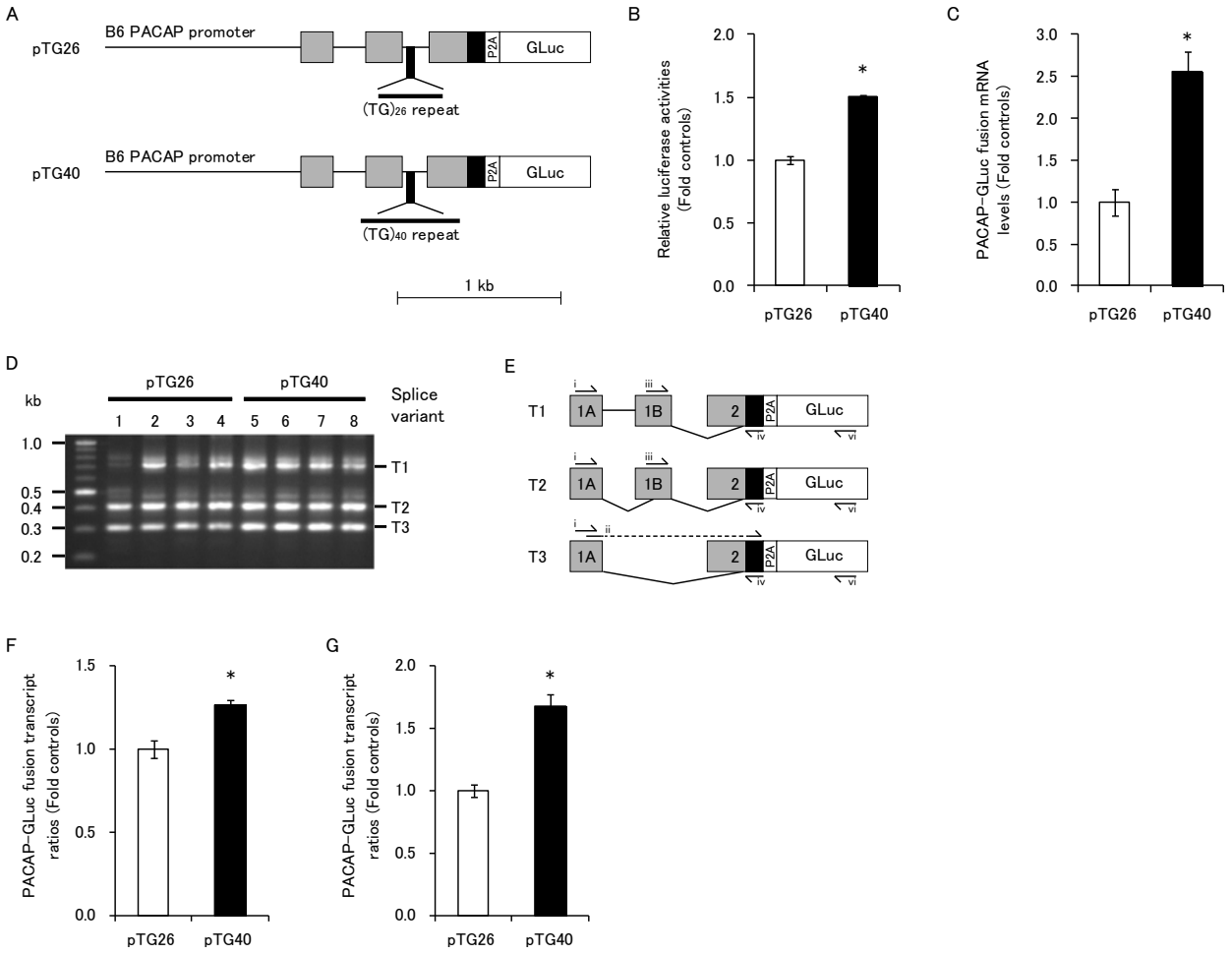

Figure 10. PACAP splice variant 3 mRNA levels depend on TG repeat lengths in second intron. (A) Schematic representation of PACAP-GLuc fusion gene constructs (pTG26 and pTG40) carrying 2.2-kb promoter sequence containing exons of the PACAP gene derived from B6 strain. GLuc reporter genes were connected to end of third exons of the PACAP gene through a self-cleaving viral sequence (P2A) sequence. Position of the sequence replaced by dinucleotide TG repeat sequence derived from MSM is shown as vertical heavy line. Relative lengths of the TG repeats are indicated as horizontal heavy lines. The names of each construct are shown on the left. (B) Luciferase activities in PC12 cells transfected with the pTG26 and the pTG40 constructs. Each construct was transfected into PC12 cells with control pTK-CLuc vector containing a constitutive TK promoter and a CLuc gene. Supernatants were collected from the transfected PC12 cells and the luciferase activities were measured. Data were normalized to the co-transfected CLuc activity. (C) PACAP-GLuc fusion mRNA levels were measured by

quantitative real-time PCR using the total the total RNAs isolated from PC12 cells transfected with each construct. Data are normalized across samples against the co-transfected CLuc mRNA levels. (D) PACAP-GLuc fusion transcripts were amplified by reverse-transcript PCR using total RNAs isolated from transfected PC12 cells of each construct. The PCR products of the pTG26 (lane 1 to 4) and the pTG40 (lane 5 to 8) were electrophoresed. DNA sizes are indicated on the left. Names of PACAP-GLuc fusion splice variants corresponding to the bands were indicated on the right. (E) Schematic structures of the PACAP-GLuc fusion splice variants. Descriptions are according to Figure 8. Primer sets used for reverse-transcript PCR and quantitative real-time PCR are indicated as arrows in corresponding to the positions. Names of the PACAP-GLuc splice variants are indicated on the left. (F-G) Ratio of the PACAP-GLuc fusion splice variant T3 to T1 and T2 were measured by reverse-transcript PCR (F) and quantitative real-time PCR (G). (F) Signal densities on agarose gel were analyzed using ImageJ 1.48. (G) Total RNAs isolated from PC12 cells transfected with each construct were used. n = 4 samples/group. Data are normalized across samples against the PACAP-GLuc fusion splice variant T1 and T2. Data are presented as mean ± SEM. *$P < 0.005$ vs. pTG26 construct.

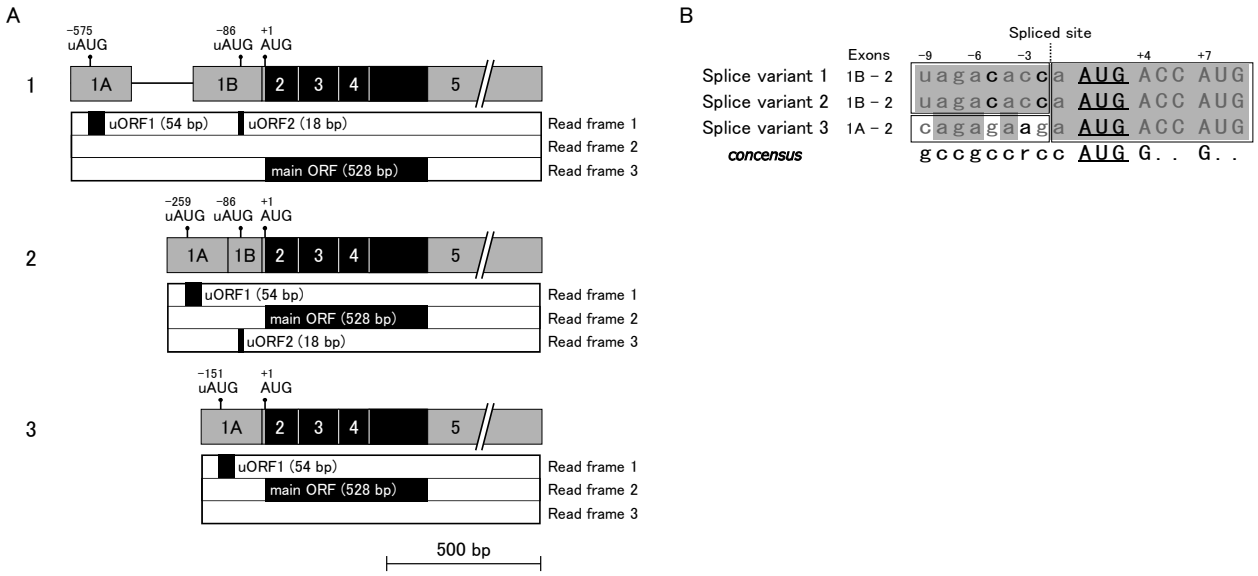

Figure 11. Structural comparison of the PACAP splice variants. (A) Schematic representation of the PACAP splice variant 1, 2, and 3. Descriptions are according to Figure 8. Positions of upstream start codons (uAUGs) are indicated as bars with distances against to start codon (AUG) of main open reading frame (ORF). Regions of the upstream open reading frames (uORFs) and the ORFs in each read frame are shown as black boxes with the lengths on the bottom of the PACAP splice variants. (B) Comparison of start codon flanking sequences of the PACAP splice variant 1, 2, and 3. The consensus (Kozak sequence) for initiation of translation is showed for purposes of comparison (r = purine (a or g) and dot = any base). Names of the PACAP splice variants and combinations of the PACAP exons are indicated on the left of nucleotide residues. Nucleotide residues in the 5' UTR are in lower-case. Nucleotide residues in common with the consensus are indicated in bold letter. Common nucleotide residues among the PACAP transcripts are boxed with grey color. Common exonic sequences among the PACAP transcripts are framed. Start codons (AUGs) are underlined.

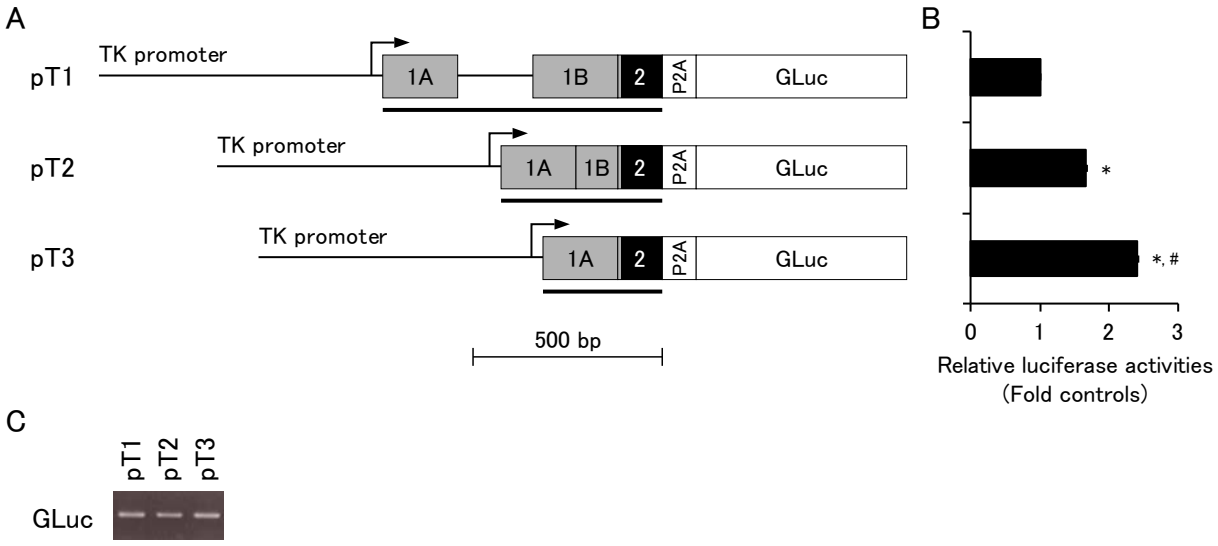

Figure 12. Translation efficiencies between PACAP-GLuc splice variants with alternate 5' UTR. (A) Schematic representation of constructs (pT1, pT2, and pT3) carrying a constitutive TK promoter sequence connected with a PACAP-GLuc fusion cDNA sequence. Descriptions are according to Figure 8. Transcription start site is indicated as an arrow on the TK promoter. Regions derived from the PACAP gene are represented as thick bars on the bottom of each construct. (B) Luciferase activities in PC12 cells transfected with pT1, pT2, and pT3 constructs. Each construct was transfected into PC12 cells with the control pTK-CLuc vector containing a constitutive TK promoter and a *Cypridina* luciferase (CLuc) gene. Supernatants were collected from the transfected PC12 cells and the luciferase activities were measured. Data are corresponding to the constructs of (A) on the left. Data were normalized to the co-transfected CLuc activity. n = 4 samples/group. Data are presented as mean ± SEM. **P* < 0.0001 vs. pT1 activity; #*P* < 0.0001 vs. pT2 activity. (C) PACAP-GLuc fusion transcript levels were measured by reverse-transcript PCR using total RNAs isolated from PC12 cells transfected with each construct.

6. Published papers

6.1. Toshiya Arakawa*, Akira Tanave* et al. (2013). A male-specific QTL for social interaction behavior in mice mapped with automated pattern detection by a hidden Markov model incorporated into newly developed freeware. J Neurosci Methods. Advanced online. doi: 10.1111/gbb.12088. *Equally contributed.

6.2. Tatsuhiko Goto, Akira Tanave et al. (2014). Selection for reluctance to avoid humans during the domestication of mice. Genes Brain Behav. 12(8): p.760-770. doi: 10.1111/gbb.12088.